Journal of Sea Research 212 (2026) 102709

Contents lists available at ScienceDirect

Journal of Sea Research

journal homepage: www.elsevier.com/locate/seares

Nearshore iron limitation in the Humboldt Current and potential impacts on toxicity and grazers

Peter von Dassow [a,b,c,*], Victor M. Aguilera [d,e], Rodrigo Torres [f,g], Catharina Alves-de-Souza [h,i], Pierre-Amaël Auger [b,j,k], Bernardo R. Broitman [l], Bernd Krock [i,m]

[a] Facultad de Ciencias Biologicas, Pontificia Universidad Católica de Chile, Santiago, Chile
[b] Instituto Milenio de Oceanografía, Universidad de Concepción, Barrio Universitario S/N, Concepción 4070112, Chile
[c] Núcleo Milenio para el Estudio de la Desoxigenación del Océano, Universidad de Concepción, Barrio Universitario S/N, Concepción 4070112, Chile
[d] Centro de Estudios Avanzados en Zonas Áridas (CEAZA), Coquimbo, Chile
[e] Facultad de Ciencias del Mar, Depto. Biología Marina, Universidad Católica del Norte, Coquimbo, Chile
[f] Centro de Investigación en Ecosistemas de la Patagonia (CIEP), Coyhaique, Chile
[g] Centro de Investigación: Dinámica de Ecosistemas Marinos de Altas Latitudes (FONDAP-IDEAL), Valdivia y Punta Arenas, Chile
[h] Departamento de Oceanografía, Facultad de Ciencias Naturales y Oceanográficas, Universidad de Concepción, Concepción, Chile
[i] Centro de Investigación Oceanográfica COPAS Coastal, Universidad de Concepción, Concepción, Chile
[j] Univ. Brest, CNRS, IRD, Ifremer, Laboratoire d'Océanographie Physique et Spatiale (LOPS), IUEM, Brest, France
[k] Escuela de Ciencias del Mar, Pontificia Universidad Católica de Valparaíso, Valparaíso, Chile
[l] Departamento de Ciencias, Facultad de Artes Liberales, Universidad Adolfo Ibañez, Viña del Mar, Chile
[m] Alfred Wegener Institut-Helmholtz Zentrum für Polar- und Meeresforschung, Bremerhaven, Germany

ARTICLE INFO

Keywords:
Humboldt current
Iron
Phytoplankton
Domoic acid

ABSTRACT

We tested for near-shore iron (Fe)-limitation of phytoplankton at the strong upwelling center at 30°S in the Humboldt Current System (Lengua de Vaca Point). Fe-amended and control microcosms showed differences in variable fluorescence consistent with Fe-limitation (dark-adapted PSII maximum quantum efficiency, functional absorption cross-section of PSII, and the time constant for quinone Q_A oxidation). Evidence for Fe-limitation was strongest at a site within 4 km from shore south of Lengua de Vaca Point, where warmer, low chlorophyll waters came onshore due to upwelling relaxation and mesoscale circulation, and weak at a site north of Lengua de Vaca Point with higher initial chlorophyll. Alleviation of Fe-limitation in waters increased chlorophyll *a*nd particulate organic nitrogen (PON) but did not significantly affect particulate organic carbon (POC) or opal. Fe-addition at another nearshore site increased opal, but not chlorophyll, PON, or POC. The diatom *Pseudo-nitzschia* sp., a potential producer of the neurotoxin domoic acid, increased upon Fe addition. Fe-stimulated domoic acid correlated with alleviation of Fe-limitation indicated by variable fluorescence. Variation in Fe supply might be important to other trophic levels in the neritic system as scallop larvae consumed Fe-stimulated phytoplankton from the site showing Fe-limitation. Results confirm Fe-limitation of primary production can occur in very nearshore waters in the Humboldt Current System where the continental shelf is exceptionally narrow. Besides stimulating phytoplankton, inputs of Fe might increase phytoplankton toxicity, affecting other trophic levels. Even neritic ecosystems in this region may be sensitive to alteration of Fe input whether due to global or local changes.

1. Introduction

Iron (Fe) is an essential micro-nutrient that, despite being one of the most abundant elements in the Earth's crust, limits phytoplankton productivity in large regions of the open ocean due to the very low solubility of Fe(III), the thermodynamically stable oxidation state of Fe in oxygenated waters (Boyd and Ellwood, 2010; Moore et al., 2013; Jiang et al., 2024). Primary productivity near the coast is often not limited by Fe due to terrigenous Fe inputs from rivers, ground waters, and aeolian deposition, as well as benthic fluxes from shallow continental shelves. However, a combination of narrow continental shelves, low riverine inputs, low rainfall, and prevailing winds can result in a mosaic of iron

* Corresponding author at: Facultad de Ciencias Biologicas, Pontificia Universidad Católica de Chile, Santiago, Chile.
E-mail address: pvondassow@uc.cl (P. von Dassow).

https://doi.org/10.1016/j.seares.2026.102709
Received 25 February 2026; Received in revised form 12 May 2026; Accepted 18 May 2026
Available online 20 May 2026

(Fe)-limited and nitrogen (N)-limited waters as observed in the California Current upwelling system (Hutchins et al., 1998; Till et al., 2019; Forsch et al., 2023).

The Humboldt Current System (HCS) in the Eastern South Pacific stands out with exceptional pelagic fish catches (Bakun and Weeks, 2008; Chavez et al., 2008; Chavez and Messié, 2009) and might also experience a mosaic of Fe-limitation. Fe-limitation of phytoplankton in offshore areas of the northern HCS has been demonstrated (Hutchins et al., 2002; DiTullio et al., 2005), and low dissolved Fe can occur within 50 km of the Peruvian coast (Gu et al., 2024). Iron can reach the coastal ocean from the sediments, through river discharges and atmospheric inputs (Boyd and Ellwood, 2010). The HCS is characterized by extensive and shallow Oxygen Minimum Zones (OMZ) associated with the southward-flowing Equatorial Subsurface Water (ESSW) (Fuenzalida et al., 2009; Silva et al., 2009; Pizarro-Koch et al., 2019), where core waters can become anoxic (Tiano et al., 2014). Dissolved Fe can accumulate when such essentially anoxic waters interact with the continental shelf, due to the greater solubility of Fe(II) compared to Fe(III), providing an Fe-source to the overlying euphotic zone through turbulence or upwelling that can exceed aeolian inputs (Homoky et al., 2012; Noffke et al., 2012; Robinson et al., 2024), However, the degree to which anoxic waters release Fe from sediments is complex (Croot et al., 2019; Plass et al., 2020) because prolonged anoxia can deplete the shelf inventory of labile Fe while H_2S can further moderate release of Fe into the water column (Noffke et al., 2012; Schlosser et al., 2018).

Despite the Coquimbo upwelling at 30°S being one of the strongest upwelling centers in the HCS (Thiel et al., 2007; Montecino and Lange, 2009), it shows lower average surface chlorophyll *a*nd primary productivity than upwelling centers to the north and south (Montecino et al., 2006). Very low Fe levels in nearshore surface waters have been attributed to an extremely narrow (<5 km) continental shelf, low rainfall, minimal river flow, and predominantly southwesterly winds which limit aeolian input (Torres and Ampuero, 2009). Additionally, the coastal subsurface oxygen deficient waters of the HCS become oxygenated as they move south along the Chilean coast, resulting in the disappearance of the subsurface nitrite max south of 25°S (Silva et al., 2009; Cornejo and Farías, 2012), potentially contributing to decreased Fe input. Bottle experiments showed that Fe-enrichment stimulated a drop in CO_2 fugacity over 5 to 7 day incubations, ranging from −32 to −234 μatm (~4% to 33%) in samples collected at 30°S nearshore (<20 km) (Torres and Ampuero, 2009).

Coastal mosaics of Fe-limitation vs. macronutrient-limitation may impact the occurrence of Harmful Algal Blooms formed by the diatom genus *Pseudo-nitzschia*, up to half of which produce the neurotoxin domoic acid (DA; the cause of amnesic shellfish poisoning) (Trainer et al., 2009, 2012; Bates et al., 2018; He et al., 2024). This genus is especially competitive in the transitions between iron-limited and replete conditions due to their production of the intracellular Fe-storage protein ferritin (Marchetti et al., 2009, 2012; Cohen et al., 2018; Lampe et al., 2018). How Fe-limitation impacts DA production is complex (Maldonado et al., 2002; Wells et al., 2005; Brunson et al., 2024). Increases in DA have been reported upon artificial Fe-fertilization (De Baar, 2005; Silver et al., 2010; Trick et al., 2010), though Fe amendment has no effect on DA in waters where diatoms are not Fe-limited (Torres et al., 2023). In Chile, the area between 30°S-27°S is a principal zone of Harmful Algal Blooms involving DA (Barría et al., 2022; Rosales et al., 2024; Secretaria Regional Ministerial de Salud, 2026).

Chile was the subject of a highly controversial marine geoengineering proposal to conduct commercial iron fertilization in coastal waters near 30°S, with the claims that this ocean "seeding" would stimulate fish production (Tollefson, 2017). Although opposition from the scientific community stalled this proposal, it motivated a push for Chile to become the 6th nation to ratify the 2013 Amendment (LP.4(8) to the 1996 Protocol (to the 1972 Convention on the prevention of marine pollution by dumping of wastes and other matter; hereafter LP) in order to provide a specific legal mechanism for regulating such activities in territorial waters (Fundación Terram and Instituto Milenio de Oceanografía, 2020). Furthermore, it renewed scientific interest in assessing the possible role of iron limitation in Chilean waters, as well as the risks that might entail.

In this study, we aimed to confirm that Fe-limitation of phytoplankton can occur in the nearshore environment. We also aimed to determine if Fe can have effects on higher trophic levels by testing domoic acid levels and whether larvae of the scallop *Argopecten purpuratus* consumed Fe-induced phytoplankton. This scallop is locally important to aquaculture and is native in subtidal zones along the coasts of Chile and Perú, where it was naturally abundant prior to severe overfishing (Stotz and González, 1997; Kluger et al., 2019).

2. Materials and methods

2.1. Satellite observations

Remotely-sensed sea surface temperature (SST) was used to drive the sampling strategy based on the evolution of coastal upwelling. MUR (Multi-scale Ultra-high Resolution; JPL MUR MEaSUREs Project, 2010) Level 4 daily SST (~1 km resolution) over October 2017 was obtained from the Physical Oceanography Distributed Active Archive Center (https://podaac.jpl.nasa.gov).

Satellite altimetry enables the monitoring of surface current patterns controlling the fate of coastal upwelling waters, e.g. filaments and eddies. The Salto/Duacs AVISO 2014 altimetry product (Duacs/AVISO, 2014) over October 2017 was obtained from the Copernicus Marine Environment Monitoring Service (http://marine.copernicus.eu).

Satellite ocean color data were used to track the evolution of phytoplankton spatial patterns associated with coastal upwelling. Backscattering varies with particle abundance while chlorophyll is also affected by physiological variability of the chl:C ratio mostly associated with light and nutrient stress (Siegel et al., 2005; Behrenfeld et al., 2016), so we used both as proxies of phytoplankton biomass. Surface chlorophyll concentration (CHL) and particulate backscattering (bbp) were taken from a merged product of the SeaWiFS, MODIS-AQUA and MERIS datasets made available over the period 1998-present by the GlobColour project (http://globcolour.info) developed in the framework of the European Space Agency Data User Element program to support global carbon cycle research. We worked with near-real time daily Level 3 binned images (~ 4 km resolution). High cloud cover during the sampling period limited the amount of valid data.

2.2. Sampling and incubations

Sampling was conducted from a rented fishing vessel (see Figs. 1–2 and Table 1 for coordinates). To sample near-surface water without metal contamination from the boat, an acid-cleaned all plastic towed fish "sipper" system at 1 m depth (Torres and Ampuero, 2009) was deployed to permit water to be pumped onboard, via an all-plastic wet-part pump, positioned 2 m from the boat hull while underway. The pumped seawater line was divided between being pumped through an Oceans Seven 304 CTD-O (Idronaut, Italy) used to measure temperature, salinity, and dissolved oxygen (O_2; with both low temperature and low O_2 used to indicate recently upwelled waters due to the presence of the OMZ) and filling of samples or filling microcosms. This system could simultaneously fill two microcosm bottles at a time, so microcosms were filled in pairs. At each of the three sites (Site 1 used in Experiment 1, Sites 2S, and 2N used in Experiment 2), four pairs of microcosms were filled. One member of each microcosm pair was randomly assigned as the control, and $FeCl_3$ was added to the other. This protocol requires that the vessel be in motion, so subsequent pairs may sample water with distinct characteristics. To account for this, we report the distance traveled during sampling at each site and rely on pairwise statistics for evaluating differences between control and Fe-amended microcosms (see below). While the goal was to sample waters recently upwelled or

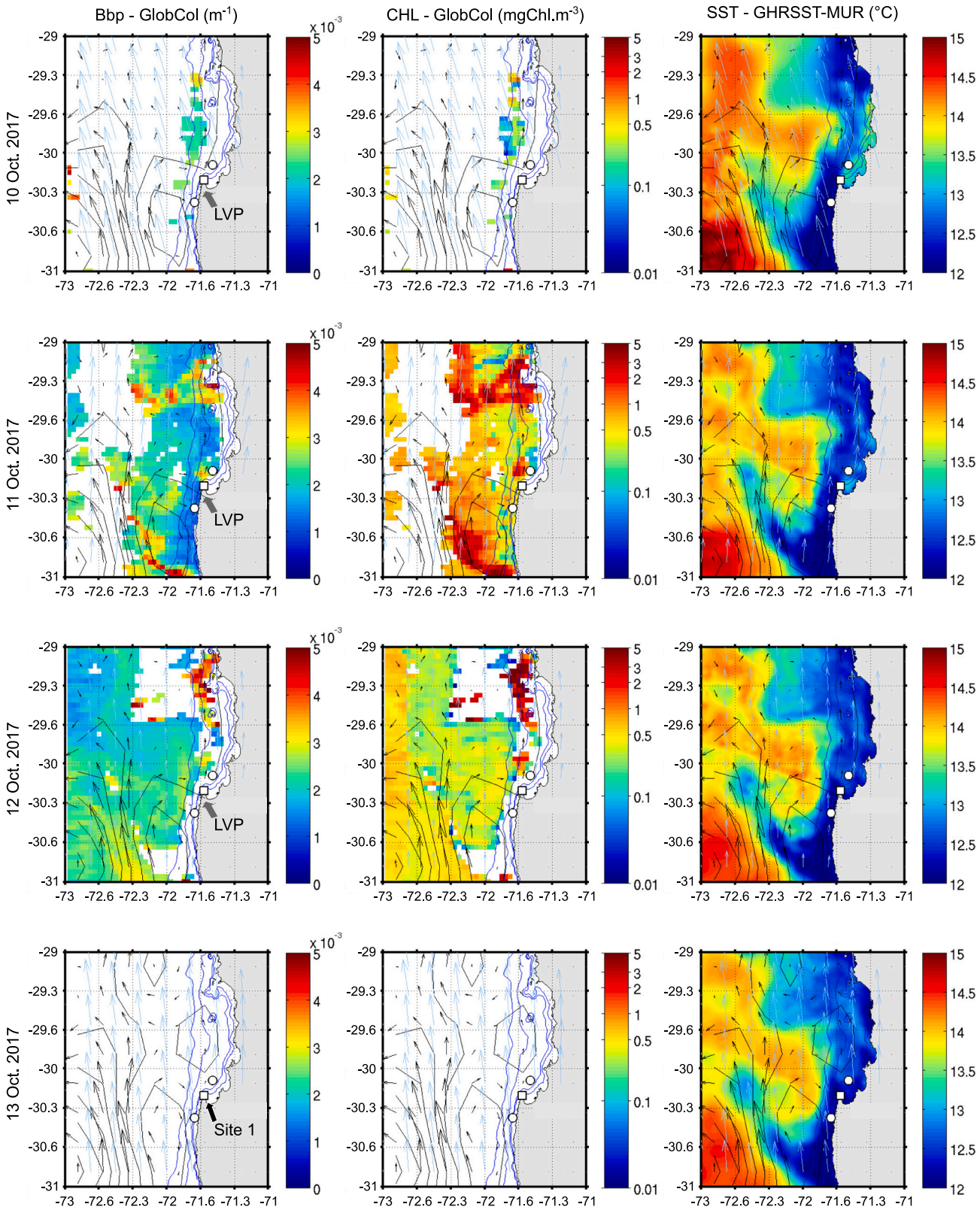

Fig. 1. Satellite observations of coastal oceanographic conditions near 30°S prior to and during the sampling on the dates 10–13 Oct. 2017 (see Fig. 2 for 14–17 Oct.). Left column panels show backscattering (bbp; m^{-1}), center panels show chlorophyll-a (CHL; mg m^{-3}) and right panels show sea surface temperature (SST; °C). Black contours and arrows indicate sea level anomaly and associated geostrophic velocities. Grey arrows represent the wind field. Blue contours are isobath 100, 200, 1000 and 2000 m. Lengua de Vaca Point (LVP) is indicated in top left panel. The white square indicates the position of Site 1 and the three CTD profiles crossing Lengua de Vaca Point, while the white circles indicate Site 2S and Site 2N. In Fig. 1 and Fig. 2, the sites are also labelled with black arrows in the left panel on the date of sampling. (For interpretation of the references to color in this figure legend, the reader is referred to the web version of this article.)

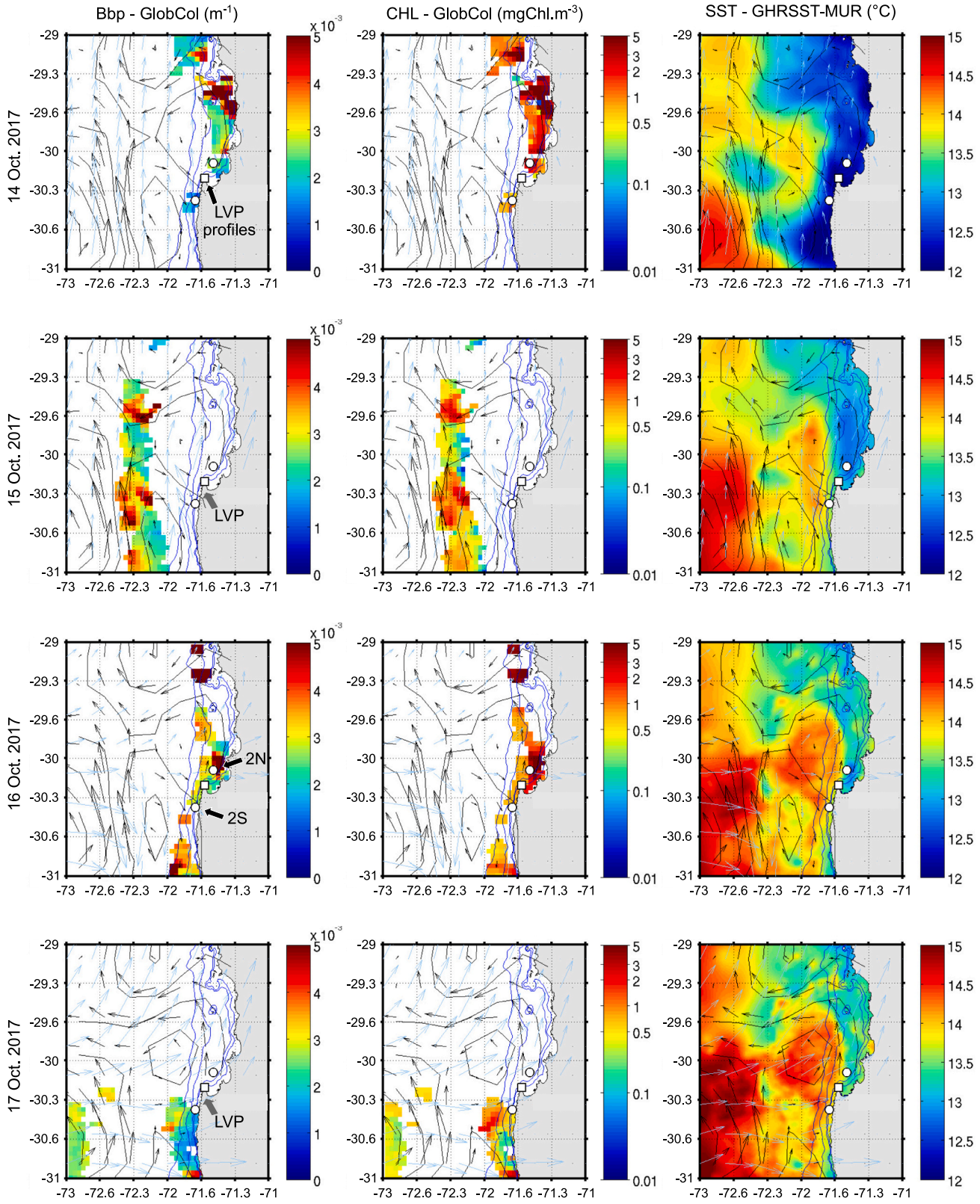

Fig. 2. As in Fig. 1, but for 14–17 Oct. 2017.

advected from offshore to the continental shelf, sampling was also affected by sea conditions (for example, on the first sampling date, conditions did not permit the vessel to leave the Bay of Tongoy).

Experiment 1 was started on 13 Oct. 2017, when sampling was performed at Site 1, near Punta Lengua de Vaca. Sampling began 1 km northwest of Punta de Lengua de Vaca (still over the continental shelf, onshore of the 200 m isobath; Fig. 1, Table 1). The towed fish had been deployed and running for 0.5 h as the vessel traveled to the start of sampling. Microcosm bottles were filled in pairs from the towed fish as the vessel was in motion, and the vessel traveled 2 km to the east over

Table 1
Coordinates of in situ sampling and measures/samples taken.

Event	Date	Latitude	Longitude	Event description
Start	13-10-2017	−30.2353	−71.6226	Deploy towed fish and water pumping
Site 1 start	13-10-2017	−30.2323	−71.6383	Start fill microcosms pairs Exp. 1
Site 1 end	13-10-2017	−30.2313	−71.6225	End fill microcosms pairs Exp. 1
Profile 1	14-10-2017	−30.2351	−71.6480	CTD profile and Niskin sample
Profile 2	14-10-2017	−30.2393	−71.6179	CTD profile and Niskin sample
Profile 3	14-10-2017	−30.2576	−71.5866	CTD profile and Niskin sample
Start	16-10-2017	−30.2198	−71.6424	Deploy towed fish and water pumping
Site 2S start	16-10-2017	−30.4111	−71.7185	Start fill microcosms pairs Exp. 2S
Site 2S end	16-10-2017	−30.4222	−71.727	End fill microcosms pairs Exp. 2S
Site 2N start	16-10-2017	−30.1096	−71.5527	Start fill microcosms pairs Exp. 2N
Site 2N end	16-10-2017	−30.0938	−71.5473	End fill microcosms pairs Exp. 2N

30 min, remaining within 1 km of the shore.

On 14 Oct. three CTD-O profiles to 20 m depth were collected near the Site 1 at Lengua de Vaca Point (located 1.8 km offshore, 0.8 km inshore, and 4.3 km inshore of the Point; Fig. 2, Table 1). In parallel, near surface samples (at 5 m or 0 m depth) were taken with a 5 L Niskin bottles for measurement of chlorophyll *a*nd domoic acid.

Experiment 2 was performed starting on 16 Oct., including microcosms filled at Site 2S, located approximately 20 km south of Punta Lengua de Vaca, and Site 2N, located at approximately 15 km north of Punta Lengua de Vaca (Table 1). The towed fish had been deployed and running for three hours as the vessel traveled to the first site (Site 2S). As microcosm pairs were filled at Site 2S, the vessel traveled 1.5 km in the direction south-southwest over 16 min. As microcosm pairs were filled at Site 2S, the vessel traveled 1.5 km in the direction south-southwest over 16 min. The distance to the nearest shore increased from 2.8 km (just offshore of the 200 m isobath) when the first bottle pair was filled, to 3.8 km when the last pair was filled. The towed fish remained deployed and running as the vessel traveled to Site 2N. At Site 2N, the distance from the coast increased from 11.1 km when the first microcosm pair was filled, to 12.3 km when the last pair was filled.

Incubations were performed in climate-controlled rooms. Temperature was set at 13 °C, and illumination was provided by cool-white fluorescent lamps with a 12:12 light-dark cycle. It was not possible to measure illumination directly, but the same lamps in a similar position provide approximately 50 μmol photons m^{-2} s^{-1}. The incubation period was four days for Site 1 and adjusted down to three days for Sites 2S and 2N because of the dense biomass reached in Experiment 1. At the end of the incubation period, microcosms were opened and samples were taken.

2.3. Variable fluorescence

Variable fluorescence was measured with a FIRe fluorometer system (Satlantic) using the blue LED. Preliminary measurements were used to establish gains, STF length, and number of repetitions following manufacturer's recommendations. FIRe data are only available from Experiment 2 due to instrument error in Experiment 1.

2.4. Biogeochemical variables

Samples (150 mL duplicated) were filtered on GF/F filters for analysis of chlorophyll *a* (chl-a). Fluorescence of acetone extracts was measured before and after acidification (Strickland and Parsons, 1984; Aminot and Rey, 2000), using an AquaFluor fluorometer with the extracted chlorophyll optical kit (Turner Designs). Only uncorrected chl-a values are reported here. The correction for phaeopigments after acidification assumes that chlorophyll-b is absent, but prasinophytes can be important in coastal waters (Collado-Fabbri et al., 2011). Nevertheless, the results for corrected chl-a were very similar.

Samples (200 mL, duplicated) were filtered on combusted GF/F filters for particulate organic carbon (POC) and particulate organic nitrogen (PON), dried, and analyzed after acidification to remove inorganic carbon by a Delta Advantage mass spectrometer coupled to a Flash EA2000 Elemental Analyzer (Thermo). This analysis was performed by the Laboratorio de Biogeoquímica e Isótopos Estables Aplicados of the Pontificia Universidad Católica de Chile). Samples for opal (particulate Si) were filtered onto 2 μm filters (200 mL, duplicated) and analyzed as in Torres et al. (2023). Samples for nutrient analysis were lost.

2.5. Phytoplankton analysis

Samples for flow cytometry (1.8 mL) in cryovials were fixed by adding 200 μL of a solution of 0.5% glutaraldehyde, 10% formaldehyde (prepared by dissolving paraformaldehyde at 60 °C), and 100 mM sodium borate pH 8.5. The fixative stock was kept frozen until use to minimize degradation of formaldehyde. After 15 min of incubation in the dark, samples were flash-frozen in liquid N_2. Samples were thawed and analyzed using an Influx Mariner Flow Cytometer as in Spilling et al. (2019).

Samples for enumeration of microphytoplankton were fixed with Lugol's and counted after Utermohl sedimentation, with identification to genus-level. *Pseudo-nitzschia* cells were further distinguished by valve width. "Small" *Pseudo-nitzschia*, with valve widths about 3 μm or less, mostly comprise species of the "*delicatissima*" and "*pseudodelicatissima*" species-complex, while those with valve widths >4 μm are likely members of the *seriata/australis* ("*seriata*") group, which mostly corresponds to *P. australis* in the studied zone (Lundholm et al., 2002; Von Dassow et al., 2023). Many samples for microphytoplankton counts were lost during shipping, so only surviving pairs are presented.

2.6. Determination of domoic acid (DA)

Cell pellets were suspended with 250 μL methanol/0.03 M acetic acid (8:2 (*v*/v)) and transferred into cryovials. The sample vial was rinsed a second time with 250 μL extraction solvent and combined with the suspension. After addition of 0.9 g lysing maxtrix D (Thermo-Savant, Illkirch, France), samples were homogenized by reciprocal shaking for 45 s at 6.5 m s^{-1} (FastPrep instrument, Thermo-Savant). The homogenates were centrifuged for 0.5 min at 7.000 ×g and supernatants were collected. Filters were transferred into 50-mL centrifugation tubes and covered with 5 mL methanol/0.03 M acetic acid (8:2 (v/v)). Homogenization of samples was achieved by two rounds of ultra-sonication with a sonotrode (Sonoplus HD2070, Bandelin, Berlin, Germany), 1 min each (cycle: 7, power: 50%). The extract was transferred to a 5-mLvial and taken to dryness in a gentle nitrogen stream. Dry samples were taken up in 500 μL methanol/0.03 M acetic acid (8:2 (v/v)). All extracts were filtered through 0.45 μm cut-off centrifugation filters (Ultrafree, Millipore, Eschborn, Germany) and filtrates were transferred to HPLC vials and stored at −20 °C until analysis.

DA was determined by liquid chromatography coupled to tandem mass spectrometry (LC-MS/MS) in the selected reaction monitoring (SRM) mode as detailed previously (Krock et al., 2008). In brief, separation was performed on a C8 column (HyperClone 3 μm BDS, 130 Å, 50 × 2 mm) with a gradient elution of water and acetonitrile, both containing 50 mM formic acid and 2 mM ammonium formate. DA was calibrated against an external calibration curve consisting of DA standard solutions (CRM programme, Institute of Marine Biology-NRC,

Halifax, NS, Canada) of 10, 50, and 100 pg μL^{-1}.

2.7. Larval growth experiments

Scallop larvae (*Argopecten purpuratus*) were kindly provided by the hatchery of Invertec (Ostimar S.A., Tongoy, Chile) at an abundance of 6 individuals mL^{-1}. After the initial incubation to assess Fe-limitation of phytoplankton growth, water was collected from pairs of microcosm bottles (Fe-amended and control) and used to fill 250 mL borosilicate glass bottles to which 60 larvae were added. Incubations were for 24 h, a time selected to be sufficient to capture clearance rates before ontogenetic changes or starvation-induced mortality confound the results (Sprung, 1984; Rico-Villa et al., 2009). The first three microcosm bottle pairs were chosen from Site 1 in Experiment 1. From Experiment 2, the first three microcosm bottle pairs were taken only from Site 2S (limitations of space and available larvae meant only one site could be selected, and Site 2S was selected because stimulation of phytoplankton by Fe was clear in bottles from that site, as described in Results). Two borosilicate bottles were filled from each microcosm bottle, one without larvae and one to which larvae were added. Larval size was measured initially and again at the end (measuring 10 larvae per bottle with a stereomicroscope, for a total of 30 per treatment). In Experiment 2, the proportions of live to dead larvae (in a minimum of 34 larvae) and the final chl-a were also measured after 24 h. Chl-a data are available only from Experiment 2. Chlorophyll-specific growth was calculated as the natural log of final vs initial chl-a, and chlorophyll-specific grazing loss was calculated as the difference with vs without larvae ($\ln(\text{chl-a}_{\text{final-w-larvae}}/\text{chl-a}_{\text{initial}})-\ln(\text{chl-a}_{\text{final-wo-larvae}}/\text{chl-a}_{\text{initial}})$).

2.8. Statistical analysis

Statistical tests were performed in Prism 10 (Graphpad, La Jolla, CA, USA). As microcosm bottles were filled in pairs and could not be sampled at time 0, the values for initial time points, when presented, are from samples taken from the towed fish system immediately prior and immediately after microcosm pairs were filled. Thus, they are not exact matches to the final microcosms, so statistical analyses only consider the values from microcosm pairs (control vs Fe-amended) at the end of the incubation. Prior to statistical tests, ratios which can only vary between 0 and 1 (Fv/Fm) were arcsine transformed while other ratios (e.g. POC/PON) and parameters which showed large consistent differences between sites were log transformed. Statistical analyses in Experiment 1 evaluated differences in chl-a, POC, PON between control and Fe-amended microcosms using paired *t*-tests. In Experiment 2, matched 2-way ANOVAs were used, including testing effects of treatment × site, treatment, site, and pair. When significant differences were detected either in treatment or treatment × site, Sídák posthoc testing was used to determine which site (N o S) showed significant differences between control and Fe-amended treatments. To test whether differences in DA between control and Fe-amended treatments correlated with differences in Fv/Fm, a simple linear regression was performed.

3. Results

3.1. Oceanographic conditions before and during sampling periods

Upwelling favorable winds were present from 6 to 13 Oct. 2017 (Figs. 1–2). From 7 to 14 October, satellite data showed cooler recently upwelled water (<13 °C) persisted nearshore and in a jet extending offshore from south of Lengua de Vaca Point (Figs. 1–2). Upwelling relaxation began on 14 Oct., and on 15–16 Oct. warmer waters came onshore (Fig. 2). However, geostrophic currents (from satellite altimetry) indicated persistent onshore flow affecting Lengua de Vaca Point itself throughout the study period (Figs. 1–2). An increase in coastal phytoplankton biomass very nearshore was indicated by both bbp and CHL signals on 16 October (Fig. 2) compared to 11–12 Oct. (Fig. 1), although cloud cover limited signals from the study area. South of Lengua de Vaca Point on 17 Oct., bbp and CHL suggested phytoplankton biomass dropped further (Fig. 2).

On 13 Oct., a 1.56 km transect from east to west was made 0.6 km to the north of Lengua de Vaca Point prior to sampling from Site 1. Sea surface temperature (SST) varied from 11.6 to 11.9 °C (consistent with satellite imagery and active coastal upwelling), sea surface salinity (SSS) remained at 34.5, and dissolved O_2 varied from 3.09 to 5.33 mg L^{-1}. Sampling at Site 1 was performed immediately after a transect in the reverse direction, during which SST ranged from 11.6 to 12.0 °C, salinity remained at 34.5. Dissolved O_2 varied from 3.01 to 3.80 mg L^{-1}, being lowest at the start of sampling. In situ biomass values varied from 0.72 to 0.76 μg L^{-1} chl-a, 27–29 μmol C L^{-1} POC, 3.1–3.4 μmol C L^{-1} PON, and 0.9–1.3 μmol Si L^{-1} opal. The phytoplankton community contained abundant diatoms (>20 cells mL^{-1}) from the centric genera *Chaetoceros*, *Detonulla*, and *Skeletonema* and the pennate genera *Asterionella* and *Pseudo-nitzschia* (Table 3).

On 14 Oct., three points were sampled around Lengua de Vaca Point, profiling down to 20 m. Temperature did not vary over this depth range, staying at 11.6 °C west (offshore) of the Point and 11.7 °C east (inshore) of the Point. Dissolved O_2 dropped from 4.17 mg L^{-1} (offshore) and 3.38 mg L^{-1} (inshore) at the surface to 2.83 mg L^{-1} (offshore) and 2.46 mg L^{-1} (inshore) at 20 m depth. Surface chl-a was 0.51 ± 0.01 μg L^{-1}. In this transect, in situ DA was measured, ranging from 1.3 to 1.7 ng L^{-1}.

On 16 Oct., during sampling at Site 2S, SST ranged from 13.6 to 13.8 °C while salinity remained at 34.3, suggesting a water mass coming from the open ocean. Dissolved O_2 varied from 9.89 to 10.11 mg L^{-1}, with the lowest value corresponding to the first bottle pair (the rest were above 10 mg L^{-1}). During sampling at Site 2N, SST ranged from 12.6 to 13.3 °C while salinity remained at 34.3, suggesting a water mass still under coastal upwelling influence. Dissolved O_2 varied from 6.35 to 7.58 mg L^{-1} but did not vary in an obvious way with respect to SST. In situ measurement of chl-a and POC showed differences between Site 2S and Site 2N consistent with satellite observations of bbp and CHL: Chl-a values were lower at Site 2S compared to Site 2N (0.37–0.40 vs. 1.08–1.19 μg L^{-1}, respectively). Likewise, POC values were lower in Site 2S compared to Site 2N (23.7–27.0 vs 29.1–32.8 μmol C L^{-1}). In contrast, PON and opal values overlapped between Site 2S and Site 2N (3.1–4.1 vs 3.9–4.5 μmol N L^{-1} and 0.8–9.9 vs 2.6–4.9 μmol Si L^{-1}).

3.2. Experiment 1

Chl-a values increased to 3.0–5.6 μg L^{-1} by the end of the bottle incubations (between 4.1-fold to 7.6-fold higher; Fig. 3A). There were no differences in chl-a between Fe-amended and control microcosms (Table 2). In the same incubation, POC increased to 146–374 μmol C L^{-1}, with no differences between control and Fe-amended microcosms (Fig. 3B, Table 2). PON increased to 14.6–16.5 μmol C L^{-1} in control bottles and 16.7–19.2 μmol C L^{-1} in Fe-amended microcosms, being higher in the Fe-amended microcosm in every pair, although this difference was not significant (Fig. 3C). Biological opal and opal/POC increased significantly more in Fe-amended than control bottles (Fig. 3D,F). POC/PON varied widely and there was no trend in POC/PON in control vs Fe-amended microcosms (Fig. 3E). DA values were not significantly higher in Fe-amended bottles (26.4 ± 18.9 ng L^{-1}) compared to controls (22.7 ± 12.1 ng L^{-1}; Table 2).

In all microcosms, centric diatoms showed the largest numerical increases, with the genera *Chaetoceros*, *Skeletonema*, and *Detonulla* comprising the first, second, and third most numerically abundant genera, respectively, at the end of the incubation (Table 3). Among pennate diatoms, *Asterionella glacialis*, small *Pseudo-nitzschia* (assumed to belong within the diverse *P. "delicatissima"* and *P. "pseudodelicatissima"* species-complex, which are not distinguishable by light microscopy) and other smaller pennate diatoms also showed substantial increases. Only medium-sized *Chaetoceros* and larger *Pseudo-nitzschia* ("seriata" type, which are likely to be *P. australis* or the

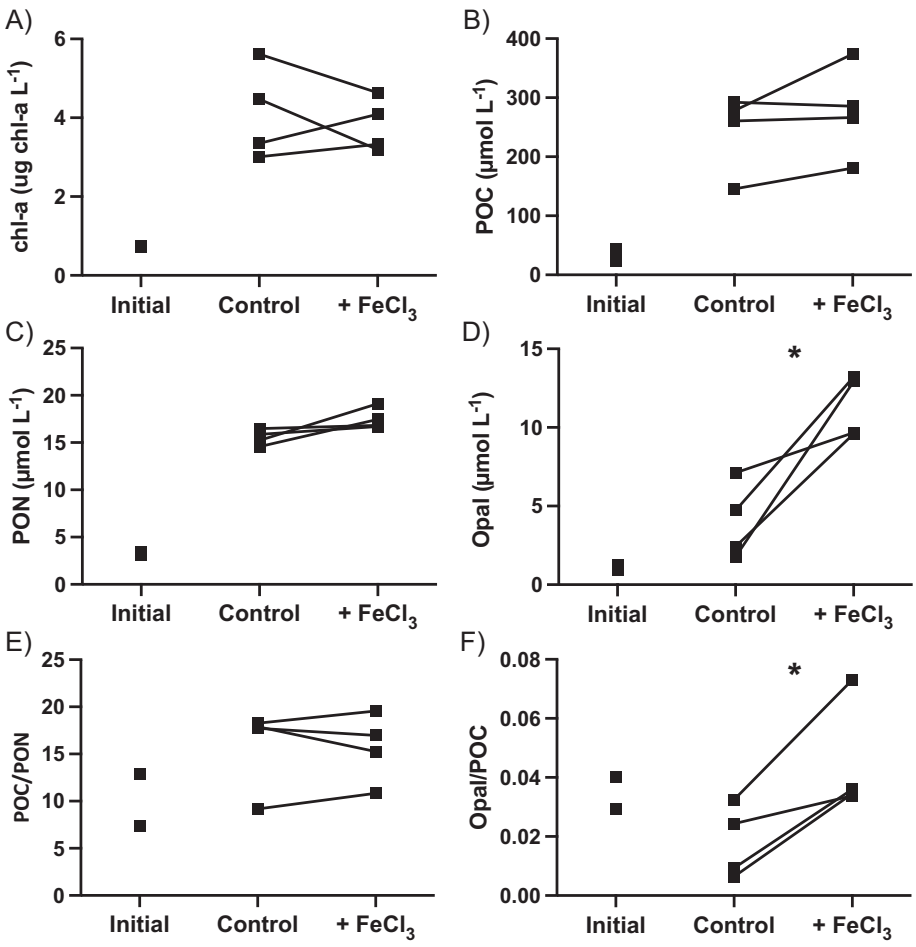

Fig. 3. Biomass response to Fe-addition in microcosm pairs from Site 1. A) Chl-a. B) POC. C) PON. D) Opal. E) POC/PON (mole/mol). F) Opal/POC (mole/mol). The values for each microcosm are shown and pairs (for comparing control-treatment) are indicated by lines. Statistical analysis is only done on control-treatment pairs as only pairs of microcosms could be filled during sampling of surface waters from the vessel, so initial conditions (time 0) bottles were collected just before and just after the sampling of the four experimental microcosm pairs. Significance of differences between control vs. Fe-amended treatments by paired *t*-tests ($p < 0.05$) are indicated by an asterisk (*).

Table 2
Results of paired t-tests for differences between control and Fe-amended microcosms in Experiment 1 (four paired microcosms). Significant differences are marked with *.

Parameter	*t*	*p*
Chl-a	0.613	0.584
POC	1.431	0.248
PON	2.369	0.099
Opal *	4.086	0.027
POC/PON	0.115	0.916
Opal/POC *	3.497	0.040
Domoic acid	0.252	0.812

P. fraudulenta) were consistently higher in the Fe-amended member of each microcosm pair (Table 3).

After the initial 4-day incubation, larvae were inoculated into water from control and Fe-amended microcosms and incubated for 1 day. Larvae size did not change significantly during the incubation (from 182 ± 6 µm, range 170–195 µm, to 183 ± 7 µm, range 170–200 µm), and there were no significant differences in larval size between larvae incubated in control vs Fe-amended water (Supplementary Fig. S1).

3.3. Experiment 2

At the end of a 3-day incubation, maximum PSII quantum efficiency (Fv/Fm) was highly variable among microcosms, but Fv/Fm tended to be higher in Fe-amended microcosms (Fig. 4A). The effect of treatment was significant but not the effect of site or site × treatment (ANOVA results for Experiment 2 are in Table 4). Fe-amended microcosms usually exhibited smaller functional absorption cross section σ_{PSI} (Fig. 4B). Microcosms from Site 2S always had higher σ_{PSI} compared to microcosms from Site 2N, and the effects of both site and treatment were significant. The quinone Q_A reoxidation time constant τ_{Qa} dropped in all microcosms from Site 2S and two from Site 2N, with significant effects of treatment and treatment × site (Fig. 4C).

Chl-a tended to increase more in Fe-amended than control microcosms (Fig. 5A). The effects of treatment and site were significant (Table 4). Within sites, the effect of Fe addition was only significant in bottle pairs from Site 2S. POC increased in microcosms from Site 2N, with increases similar between control and Fe-amended microcosms but remained low in pairs from Site 2S (Fig. 5B). POC tended to be slightly higher in Fe-amended microcosms from Site 2S, but this effect was not significant (Table 4). PON increased in microcosm incubations from both sites and both treatments (Fig. 5C). The increase was larger in microcosms from Site 2N. The increase in PON was modest but significantly higher in Fe-amended microcosms compared to control microcosms from Site 2S. Opal values increased substantially in microcosms from Site 2N, but not in Site 2S, and there was a significant effect of site on opal values (Fig. 5D). Values were higher in the Fe-amended microcosm compared to the control microcosm in three of four pairs

Table 3
Abundances (cells mL^{-1}) of phytoplankton enumerated by the Utermöhl method in Experiment 1. The T0 abundance is the average ± standard deviation of samples taken from the towed fish sampling system before and after filling the microcosm bottles. As there was no difference in chlorophyll values between Fe-amended and control microcosms and most taxa exhibited inconsistent differences between treatments, the mean ± standard deviation (with range) of all microcosms is given. The average ± standard deviation for the abundance ratio (Fe-amended/control) is shown for three taxa which showed consistent differences between treatments.

Taxon	Initial abundance	Final abundance	Ratio
Centric diatoms			
Chaetoceros spp. "small"	0 ± 0	1449 ± 1372 (0–3741)	
Chaetoceros spp. "medium"	93 ± 7	3034 ± 1522 (1336–5278)	1.7 ± 0.8
Chaetoceros spp. "large"	19 ± 21	967 ± 978 (90–2420)	
Detonulla pumilla	22 ± 4	1096 ± 2581 (0–6947)	
Ditylum brightwellii	0 ± 0	7 ± 12 (0–30)	
Eucampia zodiacus	7 ± 7	325 ± 600 (37–1681)	
Guinardia delicatula	0 ± 0	58 ± 152 (0–403)	
Guinardia striata	2 ± 3	0 ± 0 (0–0)	
Guinardia flacida	1 ± 1	12 ± 16 (0–36)	
Lauderia	0 ± 0	87 ± 230 (0–609)	
Leptocylindrus danicus	0 ± 0	1 ± 3 (0–9)	
Nitzschia longissima	1 ± 1	0 ± 0 (0–0)	
Odontella	0 ± 1	30 ± 76 (0–203)	
Rhizosolenia spp.	0 ± 0	0 ± 0 (0–0)	
Skeletonema spp.	20 ± 10	3151 ± 2064 (942–6146)	
Thalassiosira "median"	0 ± 0	28 ± 29 (0–81)	
Thalassiosira "large"	3 ± 1	130 ± 68 (22–206)	
Small centrics	3 ± 3	274 ± 424 (0–1117)	
Pennate diatoms			
Asterionella glacialis	53 ± 13	2739 ± 1486 (660–4810)	
Cylindrotheca closterium	10 ± 6	99 ± 125 (0–267)	<0.1
Nitzschia longissima	1 ± 1	0 ± 0 (0–0)	
Pseudo-nitzschia spp. "small"	42 ± 3	458 ± 331 (187–976)	
Pseudo-nitzschia spp. "seriata"	10 ± 6	16 ± 20 (0–45)	32.7 ± 0.9
Small pennates	9 ± 13	392 ± 685 (0–1624)	
Large pennates	0 ± 0	9 ± 16 (0–36)	
Others			
Thecate Dinoflagellates	3 ± 4	29 ± 76 (0–202)	

from Site 2S, but the effect was not significant. POC/PON ranged initially from 6.6 to 7.7 and 7.4–7.5 in Sites S and N, respectively, and dropped to 5.14 ± 0.47 in microcosms from Site 2S and 4.64 ± 0.30 in bottles from Site 2N after the incubation, with no effect of Fe-amendment (Fig. 5E, Table 4). Opal/POC was lower at Site 2S compared to 2S but did not change with Fe-amendment (Fig. 5F, Table 4).

For each microcosm pair, the differences between treatment and control in chl-a and in opal were significantly and positively related to the differences in Fv/Fm (Fig. 6). In the case of POC and PON, there were similar tendencies, but the effects were not significant (data not shown).

Analysis of pico- and nanophytoplankton by flow cytometry showed that Site 2S initially contained higher abundances of all pico- and nanophytoplankton groups compared to Site 2N (Supplementary Fig. S2, Table 4). *Prochlorococcus* abundances were low, below 10^3 cells mL^{-1} in Site 2N (Fig. S2A). Picocyanobacterial, picoeukaryotic phytoplankton, and cryptophyte abundances dropped during the incubation in bottles from Site 2S, with no consistent trends between Fe-amended and control bottles (Fig. S2B,C,F). In contrast, nanophytoplankton abundances increased in both treatments from Site 2S, but increased more in Fe-amended bottles (Fig. S2D). *Prochlorococcus*, *Synechococcus* and nanophytoeukaryotes in bottles from Site 2N tended to be modestly higher than the initial values from that site, whereas picophytoplankton and cryptophytes (Fig. S2E) were slightly lower. Nevertheless, there was no significant effect of either site or Fe-amendment. In bottles from Site 2S but not Site 2N, cellular red fluorescence values were higher in Fe-amended compared to control bottles for picophytoeukaryotes, and nanophytoeukaryotes (Fig, S2F), and the effects of both site and Fe-amendment were significant (Table 4).

Unfortunately, many samples for microphytoplankton counts were lost. However, one complete pair survived from each site (S and N; Table 5). The abundance of centric diatoms was much higher in the microcosms from Site 2N compared to Site 2S, with the genera *Chaetoceros* and *Skeletonema* being the most numerically important. In the pair from Site 2N, large *Chaetoceros*, both small and large ("*seriata*") *Pseudo-nitzschia*, and larger pennates were substantially (5- to 15-fold more abundant in the Fe-amended bottle, while *Skeletonema* spp. were more abundant in the control bottle. In the pair from Site 2S, larger ("*seriata*"-type) *Pseudo-nitzschia*, unidentified small pennates, and unidentified small centric diatoms were higher in the Fe-amended microcosm.

DA levels were significantly lower in microcosms from Site 2S compared to Site 2N in both control and Fe-amended treatments (Fig. 7A, Table 4). DA levels were on average higher in Fe-amended compared to control bottles (100 ± 116% in Site 2S and 56 ± 77% in Site 2N), but this effect did not reach the threshold for significance ($p = 0.087$). Nevertheless, when comparing across all microcosm pairs, the difference in DA correlated significantly both with the difference in Fv/Fm and σ_{PSI} between Fe-amended and control treatments (Fig. 7B).

After the initial 3-day incubation, larvae were inoculated into water from three pairs of control and Fe-amended microcosms and incubated for 1 day. Larval size changed insignificantly overall, from 157 ± 6 μm (range 150–170 μm) to 156 ± 9 μm (range 140–190 μm). Larval mortality varied from 0 to 22% (average 8.4 ± 8.6%), but no differences were observed between incubation with water from Fe-amended versus control microcosms. Larval size tended to be larger after treatment with water from Fe-amended versus control microcosms ($p = 0.049$) (Fig. S3A). When converted into growth rate, there was no significant difference (Fig. S3B), however it is noteworthy that pair 1, where there was no difference in size or growth between larvae grown on the control and Fe-amended phytoplankton, was the pair which showed no difference in variable fluorescence. In all bottles to which Fe-amended

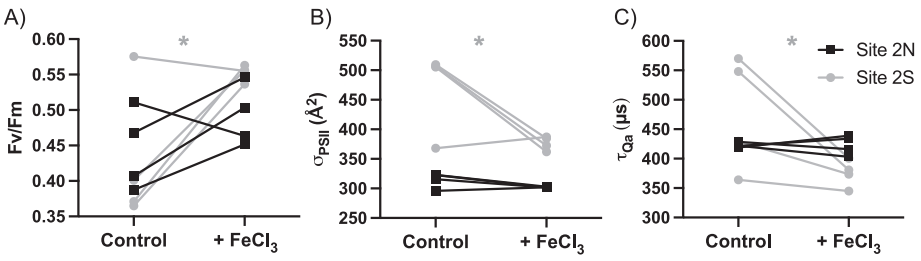

Fig. 4. Variable fluorescence parameters in microcosms from Sites 2S and 2N after 3-day incubation. Lines indicate paired microcosms (filled simultaneously at the sites). A) Maximum dark-adapted PSII quantum yield (Fv/Fm) by STF). B) Functional absorption cross section of PSII (σ_{PSII}). C) QA reoxidation time constant τ_{Qa}. Significance of differences were evaluated by paired 2-way ANOVA. Significant differences between control vs. Fe-amended treatments within a site are ($p < 0.05$) are indicated by an asterisk (grey * 2S; black * 2N).

Table 4
Results of 2-way ANOVA testing of pairwise differences between control and Fe-amended microcosms in Experiment 2. Significant differences for treatment or treatment × site are marked with *.

Parameter	Treatment × Site	Treatment	Site	Microcosm pair
Fv/Fm *[a]	$F_{1,6} = 1.686$ $p = 0.242$	$F_{1,6} = 8.448$ $p = 0.027$	$F_{1,6} = 0.602$ $p = 0.468$	$F_{6,6} = 1.183$ $p = 0.422$
σ_{PSII} *[b]	$F_{1,6} = 4.601$ $p = 0.076$	$F_{1,6} = 7.692$ $p = 0.032$	$F_{1,6} = 51.57$ $p = 0.0004$	$F_{6,6} = 0.6904$ $p = 0.668$
τ_{Qa} *[c]	$F_{1,6} = 6.768$ $p = 0.0406$	$F_{1,6} = 6.702$ $p = 0.041$	$F_{1,6} = 0.01401$ $p = 0.910$	$F_{6,6} = 2.307$ $p = 0.166$
Chl-a *[d]	$F_{1,6} = 4.197$ $p = 0.086$	$F_{1,6} = 7.943$ $p = 0.030$	$F_{1,6} = 197.7$ $p < 0.0001$	$F_{6,6} = 1.249$ $p = 0.397$
POC	$F_{1,6} = 1.442$ $p = 0.275$	$F_{1,6} = 3.414$ $p = 0.114$	$F_{1,6} = 1390$ $p = 0.0001$	$F_{6,6} = 0.6494$ $p = 0.693$
PON *[e]	$F_{1,6} = 6.512$ $p = 0.043$	$F_{1,6} = 4.944$ $p = 0.068$	$F_{1,6} = 730.7$ p = 0.0001	$F_{6,6} = 1.329$ $p = 0.369$
Opal	$F_{1,6} = 1.670$ $p = 0.244$	$F_{1,6} = 1.269$ $p = 0.303$	$F_{1,6} = 111.2$ p = 0.0001	$F_{6,6} = 5.270$ $p = 0.0315$
POC/PON	$F_{1,6} = 3.303$ $p = 0.119$	$F_{1,6} = 1.030$ $p = 0.349$	$F_{1,6} = 3.996$ $p = 0.093$	$F_{6,6} = 1.578$ $p = 0.2968$
Opal/POC	$F_{1,6} = 0.567$ $p = 0.480$	$F_{1,6} = 0.1438$ $p = 0.718$	$F_{1,6} = 28.51$ $p = 0.002$	$F_{6,6} = 4.632$ $p = 0.042$
Domoic acid	$F_{1,6} = 0.118$ $p = 0.744$	$F_{1,6} = 4.182$ $p = 0.087$	$F_{1,6} = 28.82$ p = 0.002	$F_{6,6} = 2.729$ $p = 0.124$
Prochlorococcus-like	$F_{1,6} = 1.639$ $p = 0.248$	$F_{1,6} = 1.185$ $p = 0.318$	$F_{1,6} = 7.308$ $p = 0.035$	$F_{6,6} = 0.613$ $p = 0.717$
Synechococcus-like	$F_{1,6} = 0.123$ $p = 0.738$	$F_{1,6} = 0.2078$ $p = 0.665$	$F_{1,6} = 5.183$ $p = 0.063$	$F_{6,6} = 1.194$ $p = 0.418$
Picophytoeuk.	$F_{1,6} = 0.00521$ $p = 0.945$	$F_{1,6} = 0.0489$ $p = 0.832$	$F_{1,6} = 3.089$ $p = 0.129$	$F_{6,6} = 1.746$ $p = 0.258$
Nanophytoeuk.	$F_{1,6} = 4.522$ $p = 0.078$	$F_{1,6} = 1.425$ $p = 0.278$	$F_{1,6} = 0.0176$ $p = 0.899$	$F_{6,6} = 2.140$ $p = 0.188$
Cryptophytes	$F_{1,6} = 0.342$ $p = 0.580$	$F_{1,6} = 0.2253$ $p = 0.652$	$F_{1,6} = 26.14$ p = 0.002	$F_{6,6} = 0.702$ $p = 0.661$
Picophytoeuk. red fluorescence *[f]	$F_{1,6} = 6.341$ $p = 0.045$	$F_{1,6} = 4.942$ p = 0.068	$F_{1,6} = 1.054$ $p = 0.344$	$F_{6,6} = 3.819$ $p = 0.064$
Nanophytoeuk. red fluoresc. *[g]	$F_{1,6} = 8.717$ $p = 0.026$	$F_{1,6} = 2.415$ $p = 0.171$	$F_{1,6} = 18.49$ $p = 0.005$	$F_{6,6} = 5.828$ $p = 0.025$

[a] Posthoc test showed significant difference treatment vs control in Site 2S, $p = 0.049$.
[b] Posthoc test showed significant difference treatment vs control in Site 2S, $p = 0.026$.
[c] Posthoc test showed significant difference treatment vs control in Site 2S, $p = 0.021$.
[d] Posthoc test showed significant difference treatment vs control in Site 2S, $p = 0.027$.
[e] Posthoc test showed significant difference treatment vs control in Site 2S, $p = 0.030$.
[f] Posthoc test showed significant difference treatment vs control in Site 2S, $p = 0.031$.
[g] Posthoc test showed significant difference treatment vs control in Site 2S, $p = 0.038$.

phytoplankton was added, chl-a was higher in the bottles without larvae, consistent with larval grazing, but this was not the case in some bottles filled with phytoplankton from control microcosms (Fig. 8A). Calculated grazing was modestly higher on Fe-amended microcosms (0.13–0.20 day^{-1} vs −0.18–0.06 day^{-1} in controls; Fig. 8B), but the effect was just at the significance threshold ($p = 0.05$).

4. Discussion

The current study adds to the evidence that Fe-limitation occurs in the Humboldt Current System (HCS) (Hutchins et al., 2002; DiTullio et al., 2005) even in very nearshore environments (Torres and Ampuero, 2009). To allow trace metal-clean sampling in this coastal zone, we used the towed fish "sipper" system previously employed by Torres and Ampuero (2009). The system has the advantage of being deployable from the type of small fishing vessels available to rent along the Chilean coast. However, it has the challenge of not permitting true technical replicates. Each microcosm pair was separated by approximately 300 m and may have been affected by substantial submesoscale variability in water properties. Also, we did observe variations in opal and opal/C ratios during sampling, which can also result in variability among mesocosm pairs as diatom-dominated and flagellate-dominated communities to alleviation of Fe-limitation can differ (Schulz et al., 2018).

We first consider Experiment 2, because we were able to collect variable fluorescence parameters in that experiment, which have been found to be among the most consistently sensitive to Fe-limitation as well as responding much more rapidly than other variables to the alleviation of Fe-limitation (Greene et al., 1992; Kolber et al., 1994; Behrenfeld et al., 1996, 2006; Hutchins et al., 2002; Liu and Qiu, 2012; Strzepek et al., 2012; Behrenfeld and Milligan, 2013; Trimborn et al., 2019). The three different variable fluorescence parameters measured showed consistent responses to Fe-amendment. Maximum dark-adapted PSII quantum efficiency, Fv/Fm, responded positively to addition of Fe, although the response was greater in Site 2S than in Site 2N. Fv/Fm is always reported to drop under Fe-limitation and to increase when Fe-limitation is alleviated by the addition of Fe, both in phytoplankton cultures and natural waters (citations above) although this parameter also responds to other stresses (Gorbunov and Falkowski, 2022). Functional absorption cross-section σ_{PSI} decreased as Fv/Fm increased in Fe-amended bottles. Larger σ_{PSI} under Fe-limited compared to Fe-replete conditions, and a rapid decrease in σ_{PSI} upon alleviation of Fe-limitation, has been consistently reported in diatoms, chlorophytes and the pico-cyanobacteria *Synechococcus* (Greene et al., 1992; Liu and Qiu, 2012; Strzepek et al., 2012; Trimborn et al., 2019). One study reported that this parameter increases upon Fe addition to natural phytoplankton communities in equatorial HNLC waters (Behrenfeld and Milligan, 2013), but Fe-addition to temperate HNLC waters of the North Pacific (perhaps more similar to the waters of the zone studied here) decreased σ_{PSI} (Suzuki et al., 2009), like reports in culture experiments. Such differences might reflect differences in adaptations of organisms in different habitats (Strzepek and Harrison, 2004). Here, we consider the lower σ_{PSI} in Fe-amended bottles to be consistent with alleviation of Fe-limitation. The dark-adapted Q_A reoxidation time constant τ_{Qa} is a fluorescence parameter suggested to be more specific than other variable fluorescence parameters to Fe-status than N-status, as it increases under Fe-limitation and decreases upon Fe-addition to Fe-limited phytoplankton yet is unchanged under N-stress (Greene et al., 1992; Liu and Qiu, 2012; Trimborn et al., 2019; Gorbunov and Falkowski, 2021, 2022). Consistent with detection of Fe-limitation in Experiment 2, τ_{Qa} was lower in Fe-amended microcosms in all four pairs from Site 2S, though only two from Site 2N.

Thus, all variable fluorescence parameters suggested stronger Fe-limitation in Site 2S and weaker or no Fe-limitation in Site 2N. A major weakness in our study is the lack of nutrient data due to loss of these samples as ideally nitrate and Fe concentrations would be measured to assess in situ levels as the Fe to nitrate ratio or similar

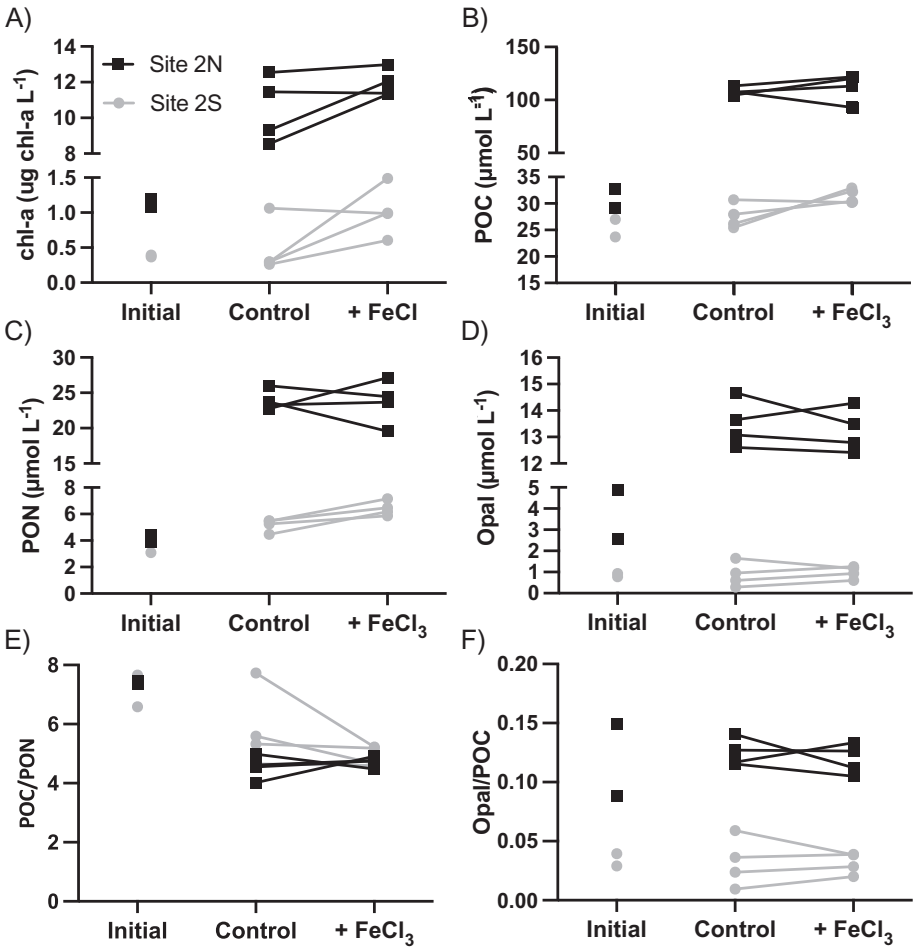

Fig. 5. Biomass response to Fe-addition in microcosm pairs from Site 2S and 2N. A) Chl-a. B) POC. C) PON. D) Opal (biogenic silicate). E) POC/PON (mole/mol), F) Opal/POC (mole/mol). The value for each microcosm is shown, and pairs (for comparing control-treatment) are indicated by lines. Significant differences between control-treatment within a site are ($p < 0.05$) are indicated by an asterisk (grey * 2S; black * 2N).

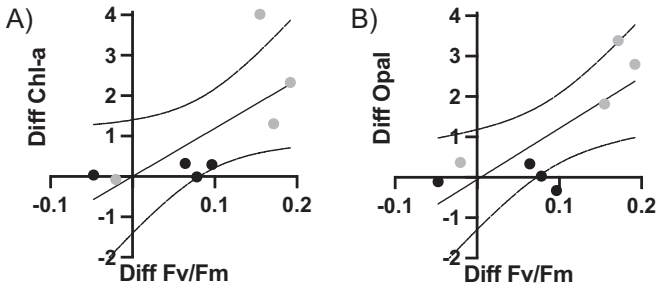

Fig. 6. The effect of treatment on chlorophyll and opal in Sites 2S and 2N correlated with the effect on variable fluorescence. Lines represent linear regression with 95% confidence intervals. A) Pairwise normalized difference in chl-a vs. difference in Fv/Fm ($R^2 = 0.50$, $p = 0.049$). B) Pairwise normalized difference in opal vs difference in Fv/Fm ($R^2 = 0.60$, $p = 0.025$).

indicators are usually used to confirm the potential for Fe limitation (Till et al., 2019). However, both sites showed SST and salinity consistent with dominance by recently upwelled Subantarctic Water, which is rich in macronutrients (Silva et al., 2009; Torres and Ampuero, 2009). Previous data from the same zone would suggest that Site 2N would have had high nutrients (in the range of 15–20 µM nitrate and silicate) (Torres and Ampuero, 2009). Site 2S had higher SST so was expected to have lower macronutrients.

Dissolved Fe tends to be much higher inland of the shelf break than farther offshore both in the California Current and Humboldt Current (Bruland et al., 2005; Kudela et al., 2006), and Torres and Ampuero (2009) concluded that Fe-limitation in recently upwelled water (low SST) in the zone studied here is most likely to occur offshore of the shelf break (200 m). Site 2S was just offshore of the 200 m isobath, much closer to the coast than Site 2N, so it may be surprising that Site 2S exhibited much stronger evidence of Fe-limitation than Site 2N.

Nevertheless, occasional reports of Fe-limited waters over the shelf in the California Current System (e.g., Hutchins et al., 2002) have been explained by upwelling relaxation causing a pause in supply of Fe from the shelf, or by mesoscale features bringing offshore water onshore (Till et al., 2019). Geostrophic velocities on 15–16 Oct. 2017 indicated Site 2N was affected by a northward current where water might have interacted with the shelf (injecting Fe) upon upwelling. Satellite altimetry and associated geostrophic velocities indicated that water at Site 2S had been advected onshore by a persistent anticyclonic circulation centered to the south of Lengua de Vaca Point during and prior to sampling at that site (Figs. 1–2). The geostrophic circulation appears consistent with the explanation of Till et al. (2019) for how Fe-limited waters can occasionally occur very near shore: Site 2S may have contained water that had been upwelled earlier to the south, advected offshore by the mesoscale feature, before any Fe could be taken up by interaction with the seafloor, and then advected onshore again (after warming) by the same mesoscale circulation. The Fe-limitation would explain the more moderate chl-a (indicated by satellite CHL and bbp as well as in situ measurement of chl-a) and that it would have retained sufficient macronutrients to exhibit phytoplankton growth upon Fe

Table 5
Abundances (cells mL^{-1}) of phytoplankton enumerated by the Utermöhl method in Experiment 2.

Taxon	Site 2S control	Site 2S Fe-amended	Site 2N control	Site 2N Fe-amended
Centric diatoms				
Chaetoceros spp. "small"	0	0	1903	1489
Chaetoceros spp. "median"	53	53	3806	3722
Chaetoceros spp. "large"	0	0	182	872
Detonulla pumilla	0	0	36	30
Ditylum brightwellii	0	0	0	0
Eucampia zodiacus	0	9	36	15
Guinardia delicatula	0	0	0	0
Guinardia striata	0	0	0	0
Guinardia flacida	0	0	18	7
Lauderia	0	0	0	0
Leptocylindrus danicus	0	0	82	52
Nitzschia longissima	0	0	0	0
Odontella	18	0	0	0
Rhizosolenia spp.	0	9	9	0
Skeletonema spp.	0	0	6253	456
Thalassiosira "median"	9	0	36	60
Thalassiosira "large"	0	0	46	15
Small centrics	9	27	0	0
Medium centrics	0	0	0	0
Pennate diatoms				
Cylindrotheca closterium	0	0	0	0
Nitzschia longissima	0	0	0	0
Pseudo-nitzschia spp. "small"	142	89	9	135
Pseudo-nitzschia spp. "seriata"	0	27	0	52
Small pennates	0	89	0	0
Large pennates	0	9	91	752

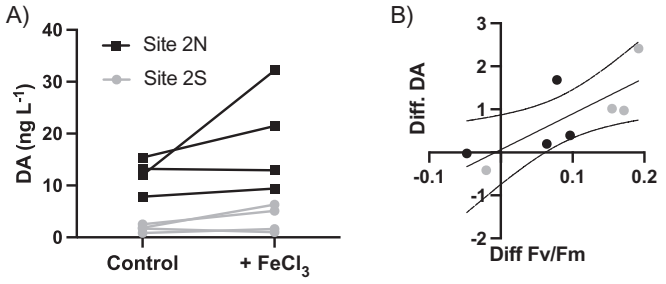

Fig. 7. A) DA levels in microcosms from Sites 2S and 2N. Microcosm pairs are indicated by lines. B) The pairwise normalized difference in DA vs difference in Fv/Fm. Lines represent linear regression with 95% confidence interval (R^2 = 0.60, p = 0.024).

amendment. This would also explain the similar salinity between Sites 2N and 2S despite higher temperatures at Site 2S. The very narrow shelf and steep slope of the continental margin in northern Chile may imply that mesoscale activity can cause even very nearshore waters to be sensitive to Fe-amendment.

Changes in chl-a paralleled changes in Fv/Fm in the bottle pairs among both Sites S and N. However, changes in POC, PON and opal were small (sometimes even negative) in Site 2S. The increase in pico- and nanophytoplankton fluorescence per cell, and the lack of consistently higher cell counts in the Fe-amended microcosm, indicated that part of the increase in chl-a may have been due to a higher chl-a per cell in Fe-amended microcosms at Site 2S. In microcosms from Site 2N, in contrast, much larger increases in chl-a were seen in control and Fe-amended microcosms and were reflected by large increases in POC, PON, opal,

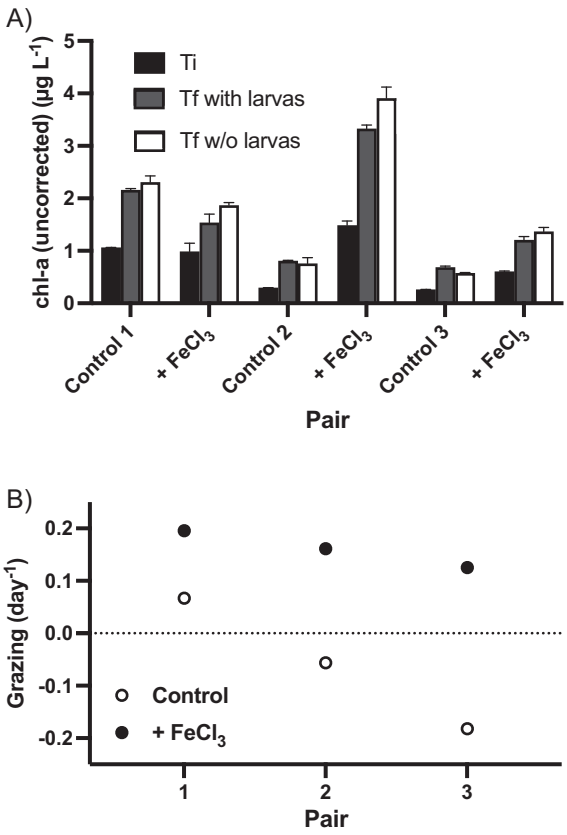

Fig. 8. Evidence for grazing by scallop larvae on phytoplankton microcosm communities. A) Chl-a levels in bottles filled with phytoplankton from control and Fe-amended microcosms from Site 2S, measured before and after incubation with and without larvae. B) Grazing rates calculated from difference in the change of hl-a with and without larvae.

and diatom abundances in microcosms. The lack of increase in picoplankton or nanoplancton abundances upon Fe-addition in both sites, in either control or Fe-amended microcosms, may be due to tight coupling with predominantly grazers that are also small-sized and respond rapidly (Landry et al., 2000b, 2000a). The higher initial biomass, a higher portion of diatoms (indicated by a higher opal/POC), and more nutrients due to more recently upwelled water permitted higher growth in Site 2N. In contrast, the low increases in biomass at Site 2S, even with Fe-amendment, suggest that the waters at this site might have been secondarily limited by macro-nutrients.

As Site 1 was very close to shore and at the entrance of Tongoy Bay, it was not expected to be Fe-limited. Indeed, pronounced increases in chl-a, POC, and PON in all microcosms, independently of Fe-amendment, were consistent with no initial nutrient limitation (unfortunately, we do not have variable fluorescence measures from this site), as would be expected from the SST below 12 °C (Torres and Ampuero, 2009). However, opal increased much more strongly in Fe-amended bottles, which might indicate that diatoms were secondarily Fe-limited in these waters.

Some lab studies report Fe-limitation restricts cellular DA production (Bates et al., 2001; Sobrinho et al., 2017), while other lab studies as well as a recent environmental metatranscritomic study indicate that DA production is strongly induced by acclimation to low Fe or to co-limitation by Fe and other nutrients (Maldonado et al., 2002; Wells et al., 2005; Brunson et al., 2024). Despite these contrasting reports, *Pseudo-nitzschia* is highly competitive for Fe (Wells et al., 2005; Marchetti et al., 2009; Trainer et al., 2009, 2012; Trick et al., 2010; Cohen et al., 2018; Lampe et al., 2018). Both *Pseudo-nitzschia* spp. and DA were detected in situ in this study as in previous studies in the zone, where

microscopy and molecular studies have reported that principal *P. "australis/seriata"*-type species present repeatedly in this zone is the highly toxic *P. australis*, while the smaller *P. pseudo-nitzschia* spp. reported in this area include both toxic and non-toxic species (Álvarez et al., 2009; Von Dassow et al., 2023). In Experiment 2, DA after microcosm incubations were substantially higher that had been measured in situ at Punto Lengua de Vaca. DA tended to be higher in Fe-amended compared to control microcosms, but differences were highly variable. This might partly reflect the variation in Fe-limitation among pairs, but it might also reflect differences in the specific phytoplankton seed communities captured in each microcosm pair, where the abundance and species of *Pseudo-nitzschia* present would be expected to be important. Nevertheless, DA was higher in Fe-amended microcosms proportionally to differences in variable fluorescence parameters between Fe-amended and control microcosms, consistent with Fe-induced DA that relates to the degree of initial Fe-limitation. In microcosm pairs for which data is available, the larger *Pseudo-nitzschia* were typically higher in the Fe-amended bottle, so the higher DA in Fe-amended treatments might be due partially to growth of these *Pseudo-nitzschia*. Pulses of Fe to Fe-limited waters, for example at the borders between Fe-poor and Fe-rich waters in in a coastal boundary region with patchy Fe concentrations, might stimulate the growth of *Pseudo-nitzschia* (over competing phytoplankton) (Trainer et al., 2012), which then increase cellular toxin levels when Fe is exhausted again enough to limit or co-limit growth.

Previous studies of microzooplankton and mesozooplankton abundances and grazing rates in response to Fe-addition focused principally on unicellular grazers or copepods (Landry et al., 2000b, 2000a; Schultes et al., 2006; Henjes et al., 2007; Chen et al., 2011). As far as we are aware, the present study is the first to look at responses of meroplanktonic invertebrates. Differences in larval growth and mortality were not detected in these short experiments. Longer-term exposure remains to be tested before concluding if Fe-induced phytoplankton would be beneficial or harmful to such larvae. Nevertheless, larvae were grazing on phytoplankton communities grown with Fe-amendment, so meroplanktonic larvae might transfer Fe-induced domoic acid to higher trophic levels.

It is striking that both this study and the study by Torres and Ampuero (2009) found that marine waters displaying Fe-limitation come within only a few kilometers from the nearby coast, an arid land that is especially rich in iron outcrops and mines (Cisternas and Gálvez, 2014), and where climate variability and human activities may affect continental sources. For instance, a megadrought since 2010 has affected glaciers, vegetation indices and land use in central and north-central Chile, including the Coquimbo Region (Boisier et al., 2025; Zambrano et al., 2025). Meanwhile, iron mining and export of iron ore are major activities that locally can generate dust (Cisternas and Gálvez, 2014; Consejo Minero, 2026). Both global and local alterations to Fe-input might impact coastal communities in this zone.

This is also the latitude of a major biogeographic and oceanographic transition (Thiel et al., 2007; Tellier et al., 2009; Tapia et al., 2014; Segovia et al., 2020) of high importance for marine conservation: The Marine Protected Areas and reserves of Damas, Choros, and Chañaral Islands at 29°S (Gutiérrez et al., 2024) are important for coastal birds such as penguins (Vianna et al., 2014) and a feeding ground for fin and blue whales (Buchan et al., 2024). The zone also has an important coastal shellfish aquaculture industry (Kluger et al., 2019; Bakit et al., 2022). Our results on the effects of Fe-amendment either on phytoplankton toxicity or on larval feeding should be considered preliminary, requiring further study. Nevertheless, the presence of near-shore pelagic Fe-limitation might be relevant to local coastal management and stakeholders.

5. Conclusions

Fe-limitation of phytoplankton can occur even in very nearshore waters of the Humboldt Current System. Variability in Fe supply to local coastal waters is an important factor in determining phytoplankton physiology, growth, composition, toxicity and quality as food for planktivorous animals.

CRediT authorship contribution statement

Peter von Dassow: Writing – review & editing, Writing – original draft, Visualization, Supervision, Resources, Project administration, Methodology, Investigation, Funding acquisition, Formal analysis, Data curation, Conceptualization. **Victor M. Aguilera:** Writing – review & editing, Resources, Methodology, Investigation, Conceptualization. **Rodrigo Torres:** Writing – review & editing, Validation, Supervision, Resources, Methodology, Investigation, Formal analysis, Data curation, Conceptualization. **Catharina Alves-de-Souza:** Writing – review & editing, Resources, Investigation, Formal analysis. **Pierre-Amaël Auger:** Writing – review & editing, Visualization, Methodology, Investigation. **Bernardo R. Broitman:** Writing – review & editing, Resources, Investigation, Conceptualization. **Bernd Krock:** Writing – review & editing, Resources, Methodology, Investigation.

Funding

This work was supported by Comisión Nacional de Investigación Científica y Tecnológica of the Chilean Ministry of Education grants FONDECYT 1141106 and FONDEQUIP EQM130267, National Agency for Research and Development (ANID) grants FONDECYT 1231703, PATSER R20F0002, ICN12_019N (Instituto Milenio de Oceanografía of Chile), and FB210021 (COPAS Coastal).

Declaration of competing interest

The authors declare that they have no known competing financial interests or personal relationships that could have appeared to influence the work reported in this paper.

Acknowledgements

We thank C. Venegas, E. Alarcón, and A. Venegas for technical support and Invertec-Ostimar S.A for provision of larvae. Two anonymous reviewers provided invaluable feedback which greatly improved the manuscript.

Appendix A. Supplementary data

Supplementary data to this article can be found online at https://doi.org/10.1016/j.seares.2026.102709.

Data availability

Data will be made available on request.

References

Álvarez, G., Uribe, E., Quijano-Scheggia, S., López-Rivera, A., Mariño, C., Blanco, J., 2009. Domoic acid production by *Pseudo-nitzschia australis* and *Pseudo-nitzschia calliantha* isolated from North Chile. Harmful Algae 8, 938–945. https://doi.org/10.1016/j.hal.2009.05.005.

Aminot, A., Rey, F., 2000. Standard procedure for the determination of chlorophyll a by spectroscopic methods. In: International Council for the Exploration of the Sea, 112, pp. 1–17.

Bakit, J., Álvarez, G., Díaz, P.A., Uribe, E., Sfeir, R., Villasante, S., et al., 2022. Disentangling environmental, economic, and technological factors driving scallop (*Argopecten purpuratus*) aquaculture in Chile. Fishes 7, 380. https://doi.org/10.3390/fishes7060380.

Bakun, A., Weeks, S.J., 2008. The marine ecosystem off Peru: what are the secrets of its fishery productivity and what might its future hold? Prog. Oceanogr. 79, 290–299. https://doi.org/10.1016/j.pocean.2008.10.027.

Barría, C., Vásquez-Calderón, P., Lizama, C., Herrera, P., Canto, A., Conejeros, P., et al., 2022. Spatial temporal expansion of harmful algal blooms in Chile: a review of 65 years records. J. Mar. Sci. Eng. 10, 1868. https://doi.org/10.3390/jmse10121868.

Bates, S.S., Léger, C., Satchwell, M., Boyer .L., G., 2001. The effects of iron and domoic acid production by *Pseudo-nitzschia multiseries*. In: Hallegraeff, G., Blackburn, S., Bolch, C.J., Lewis, R.J. (Eds.), Harmful Algal Blooms. Intergovernmental Oceanographic Commission, pp. 320–323.

Bates, S.S., Hubbard, K.A., Lundholm, N., Montresor, M., Leaw, C.P., 2018. *Pseudo-nitzschia*, Nitzschia, and domoic acid: new research since 2011. Harmful Algae 79, 3–43. https://doi.org/10.1016/j.hal.2018.06.001.

Behrenfeld, M.J., Milligan, A.J., 2013. Photophysiological expressions of iron stress in phytoplankton. Annu. Rev. Mar. Sci. 5, 217–246. https://doi.org/10.1146/annurev-marine-121211-172356.

Behrenfeld, M.J., Bale, A.J., Kolber, Z.S., Aiken, J., Falkowski, P.G., 1996. Confirmation of iron limitation of phytoplankton photosynthesis in the equatorial Pacific Ocean. Nature 383, 508–511. https://doi.org/10.1038/383508a0.

Behrenfeld, M.J., Worthington, K., Sherrell, R.M., Chavez, F.P., Strutton, P., McPhaden, M., et al., 2006. Controls on tropical Pacific Ocean productivity revealed through nutrient stress diagnostics. Nature 442, 1025–1028. https://doi.org/10.1038/nature05083.

Behrenfeld, M.J., O'Malley, R.T., Boss, E.S., Westberry, T.K., Graff, J.R., Halsey, K.H., Milligan, A.J., Siegel, D.A., Brown, M.B., 2016. Revaluating ocean warming impacts on global phytoplankton. Nat. Clim. Change 6, 323–330. https://doi.org/10.1038/nclimate2838.

Boisier, J.P., Alvarez-Garreton, C., Marinao, R., Galleguillos, M., 2025. Increasing water stress in Chile revealed by novel datasets of water availability, land use and water use. Hydrol. Earth Syst. Sci. 29, 5185–5212. https://doi.org/10.5194/hess-29-5185-2025.

Boyd, P.W., Ellwood, M.J., 2010. The biogeochemical cycle of iron in the ocean. Nat. Geosci. 3, 675–682. https://doi.org/10.1038/ngeo964.

Bruland, K.W., Rue, E.L., Smith, G.J., DiTullio, G.R., 2005. Iron, macronutrients and diatom blooms in the Peru upwelling regime: brown and blue waters of Peru. Mar. Chem. 93, 81–103. https://doi.org/10.1016/j.marchem.2004.06.011.

Brunson, J.K., Thukral, M., Ryan, J.P., Anderson, C.R., Kolody, B.C., James, C.C., et al., 2024. Molecular forecasting of domoic acid during a pervasive toxic diatom bloom. Proc. Natl. Acad. Sci. U. S. A. 121, e2319177121. https://doi.org/10.1073/pnas.2319177121.

Buchan, S.J., Ramos, M., Oyanadel, J., Santos-Carvallo, M., Bedriñana-Romano, L., Valladares, M., et al., 2024. Understanding the oceanographic dynamics of the Isla Chañaral baleen whale feeding ground, (Humboldt Archipelago, northern Chile) to extend habitat protection. Front. Mar. Sci. 10, 1208262. https://doi.org/10.3389/fmars.2023.1208262.

Chavez, F.P., Messié, M., 2009. A comparison of eastern boundary upwelling ecosystems. Prog. Oceanogr. 83, 80–96. https://doi.org/10.1016/j.pocean.2009.07.032.

Chavez, F.P., Bertrand, A., Guevara-Carrasco, R., Soler, P., Csirke, J., 2008. The northern Humboldt Current System: brief history, present status and a view towards the future. Prog. Oceanogr. 79, 95–105. https://doi.org/10.1016/j.pocean.2008.10.012.

Chen, X., Baines, S.B., Fisher, N.S., 2011. Can copepods be limited by the iron content of their food? Limnol. Oceanogr. 56, 451–460. https://doi.org/10.4319/lo.2011.56.2.0451.

Cisternas, L.A., Gálvez, E.D., 2014. Chile's mining and chemicals industries. Chem. Eng. Prog. 110, 46–51.

Cohen, N.R., Gong, W., Moran, D.M., McIlvin, M.R., Saito, M.A., Marchetti, A., 2018. Transcriptomic and proteomic responses of the oceanic diatom *Pseudo-nitzschia granii* to iron limitation. Environ. Microbiol. 20, 3109–3126. https://doi.org/10.1111/1462-2920.14386.

Collado-Fabbri, S., Vaulot, D., Ulloa, O., 2011. Structure and seasonal dynamics of the eukaryotic picophytoplankton community in a wind-driven coastal upwelling ecosystem. Limnol. Oceanogr. 56, 2334–2346. https://doi.org/10.4319/lo.2011.56.6.2334.

Consejo Minero, 2026. Cifras actualizadas de la minería. Consejo Minero. Available at https://consejominero.cl/mineria-en-chile/cifras-actualizadas-de-la-mineria/.

Cornejo, M., Farías, L., 2012. Following the N_2O consumption in the oxygen minimum zone of the eastern South Pacific. Biogeosciences 9, 3205–3212. https://doi.org/10.5194/bg-9-3205-2012.

Croot, P.L., Heller, M.I., Wuttig, K., 2019. Redox processes impacting the flux of Iron(II) from shelf sediments to the OMZ along the Peruvian shelf. ACS Earth Space Chem. 3, 537–549. https://doi.org/10.1021/acsearthspacechem.8b00203.

De Baar, H.J.W., 2005. Synthesis of iron fertilization experiments: from the iron age in the age of enlightenment. J. Geophys. Res. 110, C09S16. https://doi.org/10.1029/2004JC002601.

DiTullio, G.R., Geesey, M.E., Maucher, J.M., Alm, M.B., Riseman, S.F., Bruland, K.W., 2005. Influence of iron on algal community composition and physiological status in the Peru upwelling system. Limnol. Oceanogr. 50, 1887–1907. https://doi.org/10.4319/lo.2005.50.6.1887.

Forsch, K.O., Fulton, K.C., Weiss, M.M., Krause, J.W., Stukel, M.R., Barbeau, K.A., 2023. Iron limitation and biogeochemical effects in Southern California Current coastal upwelling filaments. JGR Oceans 128, e2023JC019961. https://doi.org/10.1029/2023JC019961.

Fuenzalida, R., Schneider, W., Garcés-Vargas, J., Bravo, L., Lange, C., 2009. Vertical and horizontal extension of the oxygen minimum zone in the eastern South Pacific Ocean. Deep-Sea Res. II Top. Stud. Oceanogr. 56, 992–1003. https://doi.org/10.1016/j.dsr2.2008.11.001.

Fundación Terram, Instituto Milenio de Oceanografía, 2020. Geoingeniería Marina: Un gran riesgo para Chile. Fundación Terram. https://www.terram.cl/descargar/documentos_en_alianza/Geoingenieria-marina-un-gran-riesgo-para-Chile.pdf (Accessed February 29, 2024).

Gorbunov, M.Y., Falkowski, P.G., 2021. Using chlorophyll fluorescence kinetics to determine photosynthesis in aquatic ecosystems. Limnol. Oceanogr. 66, 1–13. https://doi.org/10.1002/lno.11581.

Gorbunov, M.Y., Falkowski, P.G., 2022. Using chlorophyll fluorescence to determine the fate of photons absorbed by phytoplankton in the world's oceans. Annu. Rev. Mar. Sci. 14, 213–238. https://doi.org/10.1146/annurev-marine-032621-122346.

Greene, R.M., Geider, R.J., Kolber, Z., Falkowski, P.G., 1992. Iron-induced changes in light harvesting and photochemical energy conversion processes in eukaryotic marine algae. Plant Physiol. 100, 565–575. https://doi.org/10.1104/pp.100.2.565.

Gu, Y., James Hopwood, M., Gledhill, M., Rapp, I., Wuttig, K., Achterberg, E.P., 2024. Spatial and temporal variations in the micronutrient Fe across the Peruvian shelf from 1984 to 2017. Prog. Oceanogr. 221, 103208. https://doi.org/10.1016/j.pocean.2024.103208.

Gutiérrez, E., Letelier, L., Santos-Carvallo, M., Barilari, F., Gutiérrez, L., Pérez-Álvarez, M.J., et al., 2024. Zoning proposal for a marine protected area in Chile: a conservation tool for large cetaceans. Ocean Coast. Manage. 248, 106975. https://doi.org/10.1016/j.ocecoaman.2023.106975.

He, Z., Xu, Q., Chen, Y., Liu, S., Song, H., Wang, H., et al., 2024. Acquisition and evolution of the neurotoxin domoic acid biosynthesis gene cluster in *Pseudo-nitzschia* species. Commun. Biol. 7, 1378. https://doi.org/10.1038/s42003-024-07068-7.

Henjes, J., Assmy, P., Klaas, C., Verity, P., Smetacek, V., 2007. Response of microzooplankton (protists and small copepods) to an iron-induced phytoplankton bloom in the Southern Ocean (EisenEx). Deep-Sea Res. I Oceanogr. Res. Pap. 54, 363–384. https://doi.org/10.1016/j.dsr.2006.12.004.

Homoky, W.B., Severmann, S., McManus, J., Berelson, W.M., Riedel, T.E., Statham, P.J., et al., 2012. Dissolved oxygen and suspended particles regulate the benthic flux of iron from continental margins. Mar. Chem. 134–135, 59–70. https://doi.org/10.1016/j.marchem.2012.03.003.

Hutchins, D.A., DiTullio, G.R., Zhang, Y., Bruland, K.W., 1998. An iron limitation mosaic in the California upwelling regime. Limnol. Oceanogr. 43, 1037–1054. https://doi.org/10.4319/lo.1998.43.6.1037.

Hutchins, D.A., Hare, C.E., Weaver, R.S., Zhang, Y., Firme, G.F., DiTullio, G.R., et al., 2002. Phytoplankton iron limitation in the Humboldt Current and Peru Upwelling. Limnol. Oceanogr. 47, 997–1011.

Jiang, H.-B., Hutchins, D.A., Zhang, H.-R., Feng, Y.-Y., Zhang, R.-F., Sun, W.-W., et al., 2024. Complexities of regulating climate by promoting marine primary production with ocean iron fertilization. Earth Sci. Rev. 249, 104675. https://doi.org/10.1016/j.earscirev.2024.104675.

Kluger, L.C., Taylor, M.H., Wolff, M., Stotz, W., Mendo, J., 2019. From an open-access fishery to a regulated aquaculture business: the case of the most important Latin American bay scallop (*Argopecten purpuratus*). Rev. Aquac. 11, 187–203. https://doi.org/10.1111/raq.12234.

Kolber, Z.S., Barber, R.T., Coale, K.H., Fitzwateri, S.E., Greene, R.M., Johnson, K.S., et al., 1994. Iron limitation of phytoplankton photosynthesis in the equatorial Pacific Ocean. Nature 371, 145–149. https://doi.org/10.1038/371145a0.

Krock, B., Tillmann, U., John, U., Cembella, A., 2008. LC-MS-MS aboard ship: tandem mass spectrometry in the search for phycotoxins and novel toxigenic plankton from the North Sea. Anal. Bioanal. Chem. 392, 797–803. https://doi.org/10.1007/s00216-008-2221-7.

Kudela, R.M., Garfield, N., Bruland, K.W., 2006. Bio-optical signatures and biogeochemistry from intense upwelling and relaxation in coastal California. Deep Sea Research Part II. Topic. Stud. Oceanogr. 53, 2999–3022. https://doi.org/10.1016/j.dsr2.2006.07.010.

Lampe, R.H., Mann, E.L., Cohen, N.R., Till, C.P., Thamatrakoln, K., Brzezinski, M.A., et al., 2018. Different iron storage strategies among bloom-forming diatoms. Proc. Natl. Acad. Sci. U. S. A. 115. https://doi.org/10.1073/pnas.1805243115.

Landry, M., Ondrusek, M., Tanner, S., Brown, S., Constantinou, J., Bidigare, R., et al., 2000a. Biological response to iron fertilization in the eastern equatorial Pacific (IronEx II). I. Microplankton community abundances and biomass. Mar. Ecol. Prog. Ser. 201, 27–42. https://doi.org/10.3354/meps201027.

Landry, M.R., Constantinou, J., Latasa, M., Brown, S.L., Bidigare, R.R., Ondrusek, M.E., 2000b. Biological response to iron fertilization in the eastern equatorial Pacific (IronEx II). III. Dynamics of phytoplankton growth and microzooplankton grazing. Mar. Ecol. Prog. Ser. 201, 57–72.

Liu, S.-W., Qiu, B.-S., 2012. Different responses of photosynthesis and flow cytometric signals to iron limitation and nitrogen source in coastal and oceanic Synechococcus strains (Cyanophyceae). Mar. Biol. 159, 519–532. https://doi.org/10.1007/s00227-011-1832-2.

Lundholm, N., Daugbjerg, N., Moestrup, Ø., 2002. Phylogeny of the Bacillariaceae with emphasis on the genus *Pseudo-nitzschia* (Bacillariophyceae) based on partial LSU rDNA. Eur. J. Phycol. 37, 115–134. https://doi.org/10.1017/S096702620100347X.

Maldonado, M.T., Hughes, M.P., Rue, E.L., Wells, M.L., 2002. The effect of Fe and Cu on growth and domoic acid production by *Pseudo-nitzschia multiseries* and *Pseudo-nitzschia australis*. Limnol. Oceanogr. 47, 515–526. https://doi.org/10.4319/lo.2002.47.2.0515.

Marchetti, A., Parker, M.S., Moccia, Lin, E.O., Arrieta, A.L., Ribalet, F., et al., 2009. Ferritin is used for iron storage in bloom-forming marine pennate diatoms. Nature 457, 467–470. https://doi.org/10.1038/nature07539.

Marchetti, A., Schruth, D.M., Durkin, C. a, Parker, M.S., Kodner, R.B., Berthiaume, C.T., et al., 2012. Comparative metatranscriptomics identifies molecular bases for the physiological responses of phytoplankton to varying iron availability. Proc. Natl. Acad. Sci. U. S. A. 109, E317–E325. https://doi.org/10.1073/pnas.1118408109.

Montecino, V., Lange, C.B., 2009. The Humboldt Current System: ecosystem components and processes, fisheries, and sediment studies. Prog. Oceanogr. 83, 65–79. https://doi.org/10.1016/j.pocean.2009.07.041.

Montecino, V., Strub, P.T., Chavez, F., Thomas, A., Tarazona, J., Baumgartner, T., 2006. Bio-physical interactions off Western South-America. In: Robinson, A.R., Brink, K.H. (Eds.), The Sea. The Global Coastal Ocean: Interdisciplinary Regional Studies and Syntheses. Harvard University Press.

Moore, C.M., Mills, M.M., Arrigo, K.R., Berman-Frank, I., Bopp, L., Boyd, P.W., et al., 2013. Processes and patterns of oceanic nutrient limitation. Nat. Geosci. 6, 701–710. https://doi.org/10.1038/ngeo1765.

Noffke, A., Hensen, C., Sommer, S., Scholz, F., Bohlen, L., Mosch, T., et al., 2012. Benthic iron and phosphorus fluxes across the Peruvian oxygen minimum zone. Limnol. Oceanogr. 57, 851–867. https://doi.org/10.4319/lo.2012.57.3.0851.

Pizarro-Koch, M., Pizarro, O., Dewitte, B., Montes, I., Ramos, M., Paulmier, A., et al., 2019. Seasonal variability of the southern tip of the oxygen minimum zone in the eastern South Pacific (30°-38°S): a modeling study. JGR Oceans 124, 8574–8604. https://doi.org/10.1029/2019JC015201.

Plass, A., Schlosser, C., Sommer, S., Dale, A.W., Achterberg, E.P., Scholz, F., 2020. The control of hydrogen sulfide on benthic iron and cadmium fluxes in the oxygen minimum zone off Peru. Biogeosciences 17, 3685–3704. https://doi.org/10.5194/bg-17-3685-2020.

Rico-Villa, B., Pouvreau, S., Robert, R., 2009. Influence of food density and temperature on ingestion, growth and settlement of Pacific oyster larvae, *Crassostrea gigas*. Aquaculture 287, 395–401. https://doi.org/10.1016/j.aquaculture.2008.10.054.

Robinson, D., Pham, A.L.D., Yousavich, D.J., Janssen, F., Wenzhöfer, F., Arrington, E.C., et al., 2024. Iron "ore" nothing: benthic iron fluxes from the oxygen-deficient Santa Barbara Basin enhance phytoplankton productivity in surface waters. Biogeosciences 21, 773–788. https://doi.org/10.5194/bg-21-773-2024.

Rosales, S.A., Díaz, P.A., Muñoz, P., Álvarez, G., 2024. Modeling the dynamics of harmful algal bloom events in two bays from the northern Chilean upwelling system. Harmful Algae 132, 102583. https://doi.org/10.1016/j.hal.2024.102583.

Schlosser, C., Streu, P., Frank, M., Lavik, G., Croot, P.L., Dengler, M., Achterberg, E.P., 2018. H2S events in the Peruvian oxygen minimum zone facilitate enhanced dissolved Fe concentrations. Sci. Rep. 8, 12642. https://doi.org/10.1038/s41598-018-30580-w.

Schultes, S., Verity, P.G., Bathmann, U., 2006. Copepod grazing during an iron-induced diatom bloom in the Antarctic Circumpolar Current (EisenEx): I. Feeding patterns and grazing impact on prey populations. J. Exp. Mar. Biol. Ecol. 338, 16–34. https://doi.org/10.1016/j.jembe.2006.06.028.

Schulz, I., Montresor, M., Klaas, C., Assmy, P., Wolzenburg, S., Gauns, M., Sarkar, A., Thiele, S., Wolf-Gladrow, D., Naqvi, W., Smetacek, V., 2018. Remarkable structural resistance of a nanoflagellate-dominated plankton community to iron fertilization during the Southern Ocean experiment LOHAFEX. Mar. Ecol. Prog. Ser. 601, 77–95. https://doi.org/10.3354/meps12685.

Secretaria Regional Ministerial de Salud, 2026. Seremi de Salud decreta cierre preventivo por toxina amnésica en Tongoy. https://seremi4.redsalud.gob.cl/seremi-de-salud-decreta-cierre-preventivo-por-toxina-amnesica-en-tongoy/ (Accessed January 23, 2026).

Segovia, N.I., González-Wevar, C.A., Haye, P.A., 2020. Signatures of local adaptation in the spatial genetic structure of the ascidian *Pyura chilensis* along the Southeast Pacific coast. Sci. Rep. 10, 14098. https://doi.org/10.1038/s41598-020-70798-1.

Siegel, D.A., Maritorena, S., Nelson, N.B., Behrenfeld, M.J., 2005. Independence and interdependencies among global ocean color properties: reassessing the bio-optical assumption. J. Geophys. Res. 110, 2004JC002527. https://doi.org/10.1029/2004JC002527.

Silva, N., Rojas, N., Fedele, A., 2009. Water masses in the Humboldt Current System: properties, distribution, and the nitrate deficit as a chemical water mass tracer for Equatorial Subsurface Water off Chile. Deep-Sea Res. II Top. Stud. Oceanogr. 56, 1004–1020. https://doi.org/10.1016/j.dsr2.2008.12.013.

Silver, M.W., Bargu, S., Coale, S.L., Benitez-Nelson, C.R., Garcia, A.C., Roberts, K.J., et al., 2010. Toxic diatoms and domoic acid in natural and iron enriched waters of the oceanic Pacific. Proc. Natl. Acad. Sci. U. S. A. 107, 20762–20767. https://doi.org/10.1073/pnas.1006968107.

Sobrinho, B.F., De Camargo, L.M., Sandrini-Neto, L., Kleemann, C.R., Machado, E.D.C., Mafra, L.L., 2017. Growth, toxin production and allelopathic effects of *Pseudo-nitzschia* multiseries under iron-enriched conditions. Mar. Drugs 15, 331. https://doi.org/10.3390/md15100331.

Spilling, K., Camarena-Gómez, M.-T., Lipsewers, T., Martinez-Varela, A., Díaz-Rosas, F., Eronen-Rasimus, E., et al., 2019. Impacts of reduced inorganic N:P ratio on three distinct plankton communities in the Humboldt upwelling system. Mar. Biol. 166, 114. https://doi.org/10.1007/s00227-019-3561-x.

Sprung, M., 1984. Physiological energetics of mussel larvae (*Mytilus edulis*). I. Shell growth and biomass. Mar. Ecol. Prog. Ser. 17, 295–305.

Stotz, W.B., González, S.A., 1997. Abundance, growth, and production of the sea scallop *Argopecten purpuratus* (Lamarck 1819): bases for sustainable exploitation of natural scallop beds in north-central Chile. Fish. Res. 32, 173–183. https://doi.org/10.1016/S0165-7836(97)00010-6.

Strickland, J.D., Parsons, T.R., 1984. A Practical Handbook of Seawater Analysis, 2 ed. Fisheries Research Board of Canada.

Strzepek, R.F., Harrison, P.J., 2004. Photosynthetic architecture differs in coastal and oceanic diatoms. Nature 431, 689–692. https://doi.org/10.1038/nature02954.

Strzepek, R.F., Hunter, K.A., Frew, R.D., Harrison, P.J., Boyd, P.W., 2012. Iron-light interactions differ in Southern Ocean phytoplankton. Limnol. Oceanogr. 57, 1182–1200. https://doi.org/10.4319/lo.2012.57.4.1182.

Suzuki, K., Saito, H., Isada, T., Hattori-Saito, A., Kiyosawa, H., Nishioka, J., et al., 2009. Community structure and photosynthetic physiology of phytoplankton in the northwest subarctic Pacific during an in situ iron fertilization experiment (SEEDS-II). Deep-Sea Res. II Top. Stud. Oceanogr. 56, 2733–2744. https://doi.org/10.1016/j.dsr2.2009.06.001.

Tapia, F.J., Largier, J.L., Castillo, M., Wieters, E.A., Navarrete, S.A., 2014. Latitudinal discontinuity in thermal conditions along the nearshore of central-northern Chile. PloS One 9, e110841. https://doi.org/10.1371/journal.pone.0110841.

Tellier, F., Meynard, A.P., Correa, J.A., Faugeron, S., Valero, M., 2009. Phylogeographic analyses of the 30°S south-east Pacific biogeographic transition zone establish the occurrence of a sharp genetic discontinuity in the kelp *Lessonia nigrescens*: vicariance or parapatry? Mol. Phylogenet. Evol. 53, 679–693. https://doi.org/10.1016/j.ympev.2009.07.030.

Thiel, M., Macaya, E., Acu√±a, E., Arntz, W., Bastias, H., Brokordt, K., et al., 2007. The Humboldt current system of northern and central Chile: oceanographic processes, ecological interactions and socioeconomic feedback. In: Oceanogr. Mar. Biol., 45, pp. 195–344. https://doi.org/10.1201/9781420050943.ch6.

Tiano, L., Garcia-Robledo, E., Dalsgaard, T., Devol, A.H., Ward, B.B., Ulloa, O., et al., 2014. Oxygen distribution and aerobic respiration in the north and south eastern tropical Pacific Oxygen Minimum Zones. Deep-Sea Res. I Oceanogr. Res. Pap. 94, 173–183. https://doi.org/10.1016/j.dsr.2014.10.001.

Till, C.P., Solomon, J.R., Cohen, N.R., Lampe, R.H., Marchetti, A., Coale, T.H., et al., 2019. The iron limitation mosaic in the California Current System: factors governing Fe availability in the shelf/near-shelf region. Limnol. Oceanogr. 64, 109–123. https://doi.org/10.1002/lno.11022.

Tollefson, J., 2017. Plankton-boosting project in Chile sparks controversy. Nature 545, 393–394.

Torres, R., Ampuero, P., 2009. Strong CO2 outgassing from high nutrient low chlorophyll coastal waters off central Chile (30° S): the role of dissolved iron. Estuar. Coast. Shelf Sci. 83, 126–132.

Torres, R., Reid, B., Pizarro, G., Frangópulos, M., Alarcón, E., Márquez, M., et al., 2023. Iron and silicic acid addition effects on early spring macronutrient drawdown and biogenic silica production of Patagonia estuarine waters. Prog. Oceanogr. 214, 102982. https://doi.org/10.1016/j.pocean.2023.102982.

Trainer, V.L., Wells, M.L., Cochlan, W.P., Trick, C.G., Bill, B.D., Baugh, K.A., et al., 2009. An ecological study of a massive bloom of toxigenic *Pseudo-nitzschia cuspidata* off the Washington State coast. Limnol. Oceanogr. 54, 1461–1474. https://doi.org/10.4319/lo.2009.54.5.1461.

Trainer, V.L., Bates, S.S., Lundholm, N., Thessen, A.E., Cochlan, W.P., Adams, N.G., et al., 2012. *Pseudo-nitzschia* physiological ecology, phylogeny, toxicity, monitoring and impacts on ecosystem health. Harmful Algae 14, 271–300. https://doi.org/10.1016/j.hal.2011.10.025.

Trick, C.G., Bill, B.D., Cochlan, W.P., Wells, M.L., Trainer, V.L., Pickell, L.D., 2010. Iron enrichment stimulates toxic diatom production in high-nitrate, low-chlorophyll areas. Proc. Natl. Acad. Sci. 107, 5887–5892. https://doi.org/10.1073/pnas.0910579107.

Trimborn, S., Thoms, S., Bischof, K., Beszteri, S., 2019. Susceptibility of two Southern Ocean phytoplankton key species to iron limitation and high light. Front. Mar. Sci. 6, 167. https://doi.org/10.3389/fmars.2019.00167.

Vianna, J.A., Cortes, M., Ramos, B., Sallaberry-Pincheira, N., González-Acuña, D., Danta, G.P.M., et al., 2014. Changes in abundance and distribution of Humboldt penguin *Spheniscus humboldti*. Mar. Ornithol. 42, 153–159.

Von Dassow, P., Mikhno, M., Percopo, I., Orellana, V.R., Aguilera, V., Álvarez, G., et al., 2023. Diversity and toxicity of the planktonic diatom genus *Pseudo-nitzschia* from coastal and offshore waters of the Southeast Pacific, including *Pseudo-nitzschia dampieri* sp. nov. Harmful Algae 130, 102520. https://doi.org/10.1016/j.hal.2023.102520.

Wells, M.L., Trick, C.G., Cochlan, W.P., Hughes, M.P., Trainer, V.L., 2005. Domoic acid: the synergy of iron, copper, and the toxicity of diatoms. Limnol. Oceanogr. 50, 1908–1917. https://doi.org/10.4319/lo.2005.50.6.1908.

Zambrano, F., Vrieling, A., Meza, F., Duran-Llacer, I., Fernández, F., Venegas-González, A., Raab, N., Craven, D., 2025. From drought to aridification: land-cover fingerprints of a drying Chile. Earth's Fut. 13, e2025EF006744. https://doi.org/10.1029/2025EF006744.